Efficient Reduced-Basis Approximation of Scalar Nonlinear Time-Dependent Convection-Diffusion Problems, and Extension to Compressible Flow Problems

by

Han Men

Submitted to the School of Engineering
in partial fulfillment of the requirements for the degree of

Master of Science in Computation for Design and Optimization

at the

MASSACHUSETTS INSTITUTE OF TECHNOLOGY

September 2006

Author .....
School of Engineering
September, 2006

Certified by .....
Jaime Peraire
Professor of Aeronautics and Astronautics
Thesis Supervisor

Accepted by .....
Robert M. Freund
Theresa Seley Professor of Operation Research
Codirector,Computation for Design and Optimization Program

Efficient Reduced-Basis Approximation of Scalar Nonlinear Time-Dependent Convection-Diffusion Problems, and Extension to Compressible Flow Problems

by

Han Men

Submitted to the School of Engineering
on September, 2006, in partial fulfillment of the
requirements for the degree of
Master of Science in Computation for Design and Optimization

Abstract

In this thesis, the reduced-basis method is applied to nonlinear time-dependent convection-diffusion parameterized partial differential equations (PDEs). A proper orthogonal decomposition (POD) procedure is used for the construction of reduced-basis approximation for the field variables. In the presence of highly nonlinear terms, conventional reduced-basis would be inefficient and no longer superior to classical numerical approaches using advanced iterative techniques. To recover the computational advantage of the reduced-basis approach, an empirical interpolation approximation method is employed to define the coefficient-function approximation of the nonlinear terms. Next, the coefficient-function approximation is incorporated into the reduced-basis method to obtain a reduced-order model of nonlinear time-dependent parameterized convection-diffusion PDEs. Two formulations for the reduced-order models are proposed, which construct the reduced-basis space for the nonlinear functions and residual vector respectively. Finally, an offline-online procedure for rapid and inexpensive evaluation of the reduced-order model solutions and outputs, as well as associated asymptotic *a posterior* error estimators are developed. The operation count for the online stage depends only on the dimension of our reduced-basis approximation space and the dimension of our coefficient-function approximation space. The extension of the reduced-order model to a system of equations is also explored.

Thesis Supervisor: Jaime Peraire
Title: Professor of Aeronautics and Astronautics

Acknowledgments

I would first like to thank my thesis advisor Professor Jaime Peraire, for his support, encouragement and guidance during the course of my thesis work as well as my stay in MIT. I am deeply grateful for his insights, flexibility, humor and trust.

I would also like to express my deepest gratitude to Doctor Ngoc Cuong Nguyen, for his constant help, selfless teaching, invaluable suggestions and genuine encouragement throughout. I truly appreciate his patience, kindness, and care, which inspire and keep me striving for success.

I am also sincerely grateful to my colleagues, Alex Yong Kwang Tan, Revanth Reddy Garlapati, Ho Man Lui. Thanks for the many helpful and enlightening discussions on and off the topic.

Finally, above all I want to express my love and deepest appreciation to my beloved family, my parents, Chang Gui Men and Xiao Hong Huang. Your love, support and encouragement have been keeping me all the way till today and always. To them, I dedicate this thesis.

Contents

List of Figures

List of Tables

Chapter 1

Introduction

1.1 Motivation

As modern engineering design and optimization problems become progressively sophisticated both in depth and breadth, the role of mathematical modeling and numerical simulation of these problems becomes increasingly important. Often, system behavior or component attributes are modeled using governing partial differential equations (PDEs) which are in line with the underlying physics principles. Typically, the quantities of primary concern can be the *solutions* to certain field variables, — e.g., velocity, density, and pressure — or in addition, certain *outputs* which are defined as functionals of the field variables, — e.g., energy, flowrate, and temperature. These *outputs* serve to identify a certain configuration of the system parameters, or *inputs* — e.g., geometry, loads, and material properties — and are therefore modeled as functions of corresponding *inputs*.

While the solutions and outputs of the PDEs are of great importance to us, the analytical solutions to these governing equations are generally not available due to the complex nature of the systems considered, numerical procedures are sought to this end. Virtually all classical numerical approaches — e.g., finite element method (FEM)/ finite difference method (FDM)/ finite volume method (FVM) etc. — are adequate to solve the most common PDEs to the desired engineering accuracy. However, there are still problems with these standard approaches. Since they consider very *dense* approximation subspaces of the PDEs, the computational time for a particular input-output query is rather long despite the continual advance of computer speeds and expansion of hardware capacities; typical engineering design and optimization problems require considerable

number of input-output evaluations in realtime, which are not feasible to be addressed under such response time. Consequently, it is inefficient to perform any system design and optimization, robust parameter estimation of properties and states, or control of missions and processes.

Hence, the objective of this thesis is to develop a numerical approach that permits *efficient* real-time evaluation of the solutions and outputs of the PDEs and produces *certifiable* good results as compared to the classical PDE solution ("truth") approximation.

1.2 Problem Statement

Convection and diffusion arise in various engineering applications such as turbomachinery, gas and thermal dynamics, laminar and turbulent flows, viscoelastic flows, shallow water transport, and transport of contaminant in porous media. Numerical methods for convection-diffusion problems are of considerable interest in computational fluid dynamics (CFD).

In this dissertation, we will address the parameterized non-linear time-dependent convection-diffusion PDE of the following type:

$$\frac{\partial u}{\partial t} + \nabla \cdot \mathbf{f}(u) - \nu \nabla^2 u = 0, \quad \text{in } \Omega \times (0, T] \ , \tag{1.1}$$

with appropriate initial condition $u(x; \nu, t = 0) = u_0(x)$ and boundary conditions, here Ω is the closed physical domain in $\mathbb{R}^d$ with Lipschitz boundary $\partial\Omega$; and $\mathbf{f}(u) \equiv (f_1(u), \ldots, f_d(u))$, where $f_g(u)$ — a nonlinear function of the field variable u — is defined as the flux in the direction of gth coordinate. To generalize the parameter-dependence of the problem considered, the viscosity constant ν is denoted by a general parameter μ, which varies within a prescribed parameter domain $\mathcal{D} \subset \mathbb{R}$. The field variable of interest $u(x; \mu, t)$ is thus a function of the spatial coordinate x, the parameter ν, as well as the time t. Moreover, we are also concerned with certain *output* of the PDE, defined as a functional of the field variable, hence, also a function of the parameter μ and time, $s(\mu, t) = \ell(u(\mu, t))$.

In actual practice, due to infinite dimensionality, the exact solution of $u(\mu, t)$ and $s(\mu, t)$ are not obtainable. Instead, we calculate what is known as "truth" solution and output, which are the approximation of the "exact" solution and output. We henceforth introduce $X \subset X^e$, a "truth" finite element approximation space of finite but very large dimension $\mathcal{N}$. The finite element

approximation of the "exact" problem can then be restated as: given $\mu \in \mathcal{D}$, our "truth" finite element solution is now $u_h(\mu, t_k), t_k = k\Delta t, 0 \leq k \leq K \equiv T/\Delta t$, which resides in the pth-order finite element approximation space X_h^p of very large dimension $\mathcal{N}$ — Δt is a constant timestep ; thus our "truth" output becomes $s_h(\mu, t_k) = l(u_h(\mu, t_k))$. We shall assume that X_h^p is sufficiently rich and Δt is reasonably small such that $u_h(\mu, t_k)$ (respectively, $s_h(\mu, t_k)$) is sufficiently indistinguishable from $u(\mu, t)$ (respectively,$s(\mu, t)$) for all $\mu \in \mathcal{D}$ at the accuracy level of interest.

Typically, the required dimension $\mathcal{N}$ to satisfy this assumption is very large, — even with the application of appropriate adaptive mesh generation/refinement schemes — and in fact too large to perform real-time design and optimization queries effectively. The reduced-basis (RB) approximation is therefore needed and shall be built upon the "truth" finite element approximation. The evaluation of the RB approximation should also be conducted based on the comparison with this "truth" approximation.

We shall explore both finite element methods, and reduced-basis methods, as well as several model order reduction techniques in the following sections.

1.3 Literature Review

1.3.1 Finite Element Methods

Finite element methods (FEM) are most frequently used for solving PDEs that govern many engineering problems whose exact solutions by analytical techniques are very hard or even impossible to find. FEM, as a numerical method, is hence used to obtain an approximation solution. The point of departure for the FEM is a weighted-integral statement of a differential equation, called the weak formulation.

In the FEM, we seek the approximate solution over a discrete spatial domain known as triangulation $\mathcal{T}_h$ of a physical domain $\Omega : \overline{\Omega} = \bigcup_{T_h \in \mathcal{T}_h} \overline{T}_h$, where $T_h^k, k = 1, \ldots, K$, are the elements; $x_i, i = 1, \ldots, \mathcal{N}$ are the nodes, and the subscript h denoting the diameter of the triangulation $\mathcal{T}_h$ is the longest edges of all elements. We define a finite element "truth" approximation space $X_h^p \subset X^e$ as

$$X_h^p = \{v \in X^e |\ v|_{T_h} \in P^p(T_h),\ \forall T_h \in \mathcal{T}_h\} \tag{1.2}$$

where $P^p(T_h)$ is the finite element space of polynomials of order up to p^{th} over element T_h.

To obtain the discrete equation of the weak formulation, we express the field variable $u(\mu) \in X$ in terms of the nodal basic functions $\varphi_i \in X_h^p, \varphi_i(x_j) = \delta_{ij}$ such that

$$X_h^p = \text{span}\{\varphi_1, \ldots, \varphi_{\mathcal{N}}\}, \tag{1.3}$$

$$u(\mu) = \sum_{i=1}^{\mathcal{N}} u_i(\mu)\varphi_i, \quad v \in X_h^p. \tag{1.4}$$

here $u_i(\mu), i = 1, \ldots, \mathcal{N}$, is the nodal value of $u(\mu)$ at node x_i.

The spatial discretization (Triangulation) technique described above is the general approach of FEM. Depending on the connectivity of the neighboring elements and its nodes, the projections of the governing equation from "exact" space to "truth" space can be categorized into continuous Galerkin (CG) and discontinuous Galerkin (DG) methods. A large amount of works [11, 12, 7, 31] has been devoted to the development of DG methods for linear and nonlinear convection-diffusion problems recently. DG methods are highly parallelizable and can easily handle complicated geometries and boundary conditions. They are also locally conservative, high-order accurate, and are well-suited to complicated geometries and boundary conditions [12]. All these attractive properties are the main reasons for our choice of the DG methods for the numerical solution of equation (1.1).

1.3.2 Reduced-basis Methods

The reduced-basis method was first introduced in the late 1970s in nonlinear structural analysis for single parameter problems [1, 29], and subsequently abstracted and analyzed [3, 6, 16, 34, 37] and extended [19, 20, 32] to a much larger class of parameterized PDEs, and further developed more [16, 32, 34] to include *a priori* error analysis.

The reduced-basis approach is local in parameter space in both practice and theory. Later work [25, 26, 46, 28, 35, 42, 22, 13] differs from these earlier efforts in several important ways [21]: firstly, *global* approximation spaces are developed; secondly, rigorous a *posteriori* error estimators are introduced; thirdly, *offline/online* computational decompositions are exploited [3]. These three ingredients enable us to *reliably* decouple the generation and projection stages of reduced-basis approximation, thereby improving the computation cost by several orders of magnitude.

Progress has also been made in *a posteriori* error estimation for reduced-basis approximations. In particular, *a posteriori* error bounds have been successfully developed for (*i*) linear [25, 26, 46, 35,

21] and (*ii*) at most quadratically nonlinear [28, 42, 22] elliptic partial differential equations that are affine in the parameter. These enable the development of very efficient offline-online computational strategies relevant in the many-query and real-time contexts. The operation count for the online stage — in which, given a new parameter value, we calculate the reduced-basis solution and output — depends only on the parametric complexity of the problem and on the dimension of the reduced-basis space (typically much smaller), but is *independent* of the dimension of the underlying "truth" finite element approximation space (typically very large).

1.3.3 Model Order Reduction

Generally, the model order reduction (MOR) approaches can be categorized into three types: (*i*), techniques using Karhunen-Loeve expansion (or Proper Orthogonal Decomposition); (*ii*), algorithms based Krylov subspace methods; (*iii*), methods based on Hankel norm approximants and balanced truncations. The need for efficient simulation tools for dynamical (time-varying) systems arising in circuit simulation, structural dynamics and micro-electro-machanical systems is a driving force behind the development of MOR approaches. The basic idea applied by all of the approaches is a projection from high-dimensional state space to very low dimensional state space, which results in the reduced-order model of the original system. In the POD approach, probably the most popular model-order reduction technique, time is considered as the varying parameter, and "snapshots" of the field variable at different times are obtained from either a numerical or experimental procedure. The optimal approximation space is constructed by applying the singular value decomposition to these vectors, and keeping only the N vectors corresponding to the largest singular values. Since the singular values are related to the "energy" of the system, only the modes preserving the most energy are preserved. The reduced-order model is then obtained by a Galerkin projection onto the space spanned by these vectors. POD has been successfully applied in many fields: turbulent flows [24], fluid structure-interaction [14], non-linear structural mechanics [30], and turbo-machinery flows [44].

A great deal of attention has also been devoted to Krylov subspace-based methods for efficient modeling, effective realization, and fast simulation. The basic idea of these methods is to approximate the transfer function of original systems by orthogonal basis functions and projecting original systems onto that subspace [18]. Owing to their low computational cost and robustness, the Krylov

subspace-based methods have been proven very attractive for producing reduced-order model of many large-scale linear systems and have been broadly used in engineering applications: structural dynamics [2], optimal control of fluid flows [23], circuit design [10, 43], and turbomachinery [45].

In balanced truncation approach, the Hankel Singular Values (HSV) of the controllability and observability gramians of the system are computed. The state-space dimensions with low HSV are truncated, leading to a reduced-order model. For high-dimensional systems, computation of the required gramians is very expensive; combining POD and balanced truncation can overcome this limitation.

A large number of model-order reduction techniques has also been developed in particular to treat nonlinear time-dependent problems [2, 9, 8, 27, 33, 36, 40, 13]. Linearization approaches [13], for example, usually suffer from a lack of efficient representation of the nonlinear terms, whereas polynomial approximation approaches [9, 33] usually exhibit a fast exponential growth of computational complexity with the degree of the nonlinear approximation order. These two methods are thus quite expensive and do not address strong nonlinearities efficiently; other approaches for highly nonlinear systems (such as piecewise-linearization) have also been proposed [36, 39] but also at the expense of high computational cost and little control over model accuracy.

It is noted that most model-order reduction techniques focus mainly on reduced-order modeling of dynamical systems in which time is considered the *only* "variable;" the development of reduced-order models for parametric applications is much less common [41, 15].

1.4 Approach

The goal of this thesis is the rapid and reliable computations of the solution and output for nonlinear time-dependent convection-diffusion PDEs. To achieve this goal, we pursue the reduced-basis method with appropriate model reduction techniques. In our problem, both time and viscosity in equation (1.1) are treated as parameters. For convenience below, we introduce *time-discrete* sampling set $\mathbb{T} \equiv \{t_0, \ldots, t_k\}$, *parameter-time* space $\tilde{\mathcal{D}} \equiv \mathcal{D} \times \mathbb{T}$, and parameter-time variable $\tilde{\mu} \equiv (\mu, t_k) \in \tilde{\mathcal{D}}$. The foundation of the reduced basis method is the realization that the set of all solutions $u_h(\tilde{\mu})$, as $\tilde{\mu}$ varies, resides in a finite and *low dimensional* solution manifold $\mathcal{W}_h \equiv \{u_h(\tilde{\mu}) \mid \tilde{\mu} \in \tilde{\mathcal{D}}\}$. Hence, $u_h(\tilde{\mu})$ can be approximated very well by its projection $u_N(\tilde{\mu})$ on a finite vector space of N vectors $W_N^u = \text{span}\{\zeta_n \equiv u_h(\tilde{\mu}_n^u), 1 \leq n \leq N\}$, where $u_h(\tilde{\mu}_n^u), 1 \leq n \leq N$, are

the finite element (discontinuous Galerkin) solutions of equation (1.1) at N selected points in the sample $S_N^u = \{\tilde{\mu}_1^u = (\mu_1^u, t_{k_1^u}) \in \tilde{\mathcal{D}}, \ldots, \tilde{\mu}_N^u = (\mu_N^u, t_{k_N^u}) \in \tilde{\mathcal{D}}\}$.

The reduced-basis approximation approach proposed here will first build a reduced-basis approximation for the field variable. Instead of the classical Lagrangian basis $\zeta_n \equiv u_h(\tilde{\mu}_n), 1 \leq n \leq N$, we shall use a POD basis, $\Phi_N^u = \text{span}\{\phi_n, 1 \leq n \leq N\}$. In the framework of this thesis, we view POD as a "procedure" that generates a set of optimal basis functions rather than a "technique" that establishes reduced-order models.

Next, an empirical interpolation method is used to obtain inexpensive approximations for the nonlinear terms of the PDE, which then allows an efficient offline-online computational paradigm.

Two different reduced-basis formulations are then derived for the nonlinear time-dependent convection-diffusion equations. *Asymptotic a posterior* error estimators are proposed as a means to quantify the reduced-basis approximations.

The thesis begins in Chapter 2 with a description of Runge-Kutta discontinuous Galerkin (RKDG) numerical method for our nonlinear time-dependent convection diffusion PDE in equation (1.1). In Chapter 3, we present the ingredients of reduced-basis approximations, namely, the POD procedure, the Galerkin approximation, and the empirical interpolation procedure; followed by two reduced-basis formulations — function approximation and residual approximation. Extensions of the approach for the compressible Euler equations are finally discussed in Chapter 5. Numerical examples will also be presented in each chapter to access the accuracy and capability.

Chapter 2

Runge-Kutta Discontinuous Galerkin Method

In this chapter, we describe a Runge-Kutta discontinuous Galerkin method for obtaining solutions of nonlinear time-dependent convection-diffusion PDEs, upon which our reduced-basis approach is built and compared with. Two steps are involved in this method, namely, finite element space discretization by a discontinuous Galerkin approximation scheme, and a Runge-Kutta time integration scheme.

2.1 The DG Space Discretization

We first introduce a triangulation, $\mathcal{T}_h$, of the domain Ω consisting non-overlapping elements T_h, such that $\Omega = \bigcup_{T_h \in \mathcal{T}_h} T_h$; for a typical element T_h, the set of its boundary edges is denoted by $\mathcal{E}(T_h)$.

Before proceeding to derive the weak formulation for DG discretization, an auxiliary variable $\mathbf{q} = \nabla u$ is introduced. The problem in equation (1.1) is rewritten as follows

$$\begin{aligned} \frac{\partial u}{\partial t} + \nabla \cdot \mathbf{f}(u) - \mu \nabla \cdot \mathbf{q} = &\quad 0, \quad \text{in } \Omega \times (0,T] \ , \\ \mathbf{q} = &\quad \nabla u, \quad \text{in } \Omega \times (0,T] \ . \end{aligned} \tag{2.1}$$

Next, we define two spaces in which the DG solutions $(u_h, \mathbf{q}_h)$ to our finite element approxima-

tion reside,

$$X_h^p = \left\{ v \in L^2(\Omega) \quad | \quad v|_{T_h} \in P^p(T_h), \quad \forall T_h \in \mathcal{T}_h \right\}, \tag{2.2}$$

$$Y_h^p = \left\{ \mathbf{r} \in \left(L^2(\Omega)\right)^d \quad | \quad r_g|_{T_h} \in P^p(T_h), \quad \forall T_h \in \mathcal{T}_h, \ 1 \leq g \leq d \right\}, \tag{2.3}$$

where $P^p(T_h)$ is the finite element space of polynomials of order up to p^{th} over element T_h, and $L^2(\Omega)$ is the Lebesgue space of square-integrable functions over the domain $\Omega \in \mathbb{R}^d$.

By multiplying the two equations in (2.1) with test functions $v_h \in X_h^p$ and $\mathbf{r}_h \in Y_h^p$ respectively, and integrating by parts, we obtain the weak formulation of the problem: find $(u_h, \mathbf{q}_h) \in X_h^p \times Y_h^p$ such that $\forall T_h \in \mathcal{T}_h$,

$$\begin{aligned} \int_{T_h} \frac{\partial u_h}{\partial t} v_h - \int_{T_h} \mathbf{f}(u_h) \cdot \nabla v_h + \sum_{\gamma_h \in \mathcal{E}(T_h)} \int_{\gamma_h} \hat{f}(u_h, \mathbf{n}_{\gamma_h}) v_h & \\ + \mu \int_{T_h} \mathbf{q}_h \cdot \nabla v_h - \mu \sum_{\gamma_h \in \mathcal{E}(T_h)} \int_{\gamma_h} \hat{\mathbf{q}}_h \cdot \mathbf{n}_{\gamma_h} v_h &= 0, \quad v_h \in X_h^p, \end{aligned} \tag{2.4}$$

$$\int_{T_h} \mathbf{q}_h \cdot \mathbf{r}_h + \int_{T_h} u_h \nabla \cdot \mathbf{r}_h - \sum_{\gamma_h \in \mathcal{E}(T_h)} \int_{\gamma_h} \hat{u}_h \mathbf{r}_h \cdot \mathbf{n}_{\gamma_h} = 0, \quad \mathbf{r}_h \in Y_h^p. \tag{2.5}$$

where $\hat{f}(u_h, \mathbf{n}_{\gamma_h})$, $\hat{\mathbf{q}}_h$ and $\hat{u}_h$ are called numerical fluxes, and are approximations to the values of the respective functions on the boundaries $\gamma_h \in \mathcal{E}(T_h)$ of the element T_h. In DG methods, different schemes are used to evaluate these terms. For the numerical flux $\hat{f}(u_h, \mathbf{n}_{\gamma_h})$, a simple local Lax-Friedrichs flux scheme can be used,

$$\hat{f}(u_h, \mathbf{n}_{\gamma_h}) = \frac{1}{2} \left(\mathbf{f}(u_h^+) + \mathbf{f}(u_h^-) \right) \cdot \mathbf{n}_{\gamma_h} - C(u_h, \mathbf{n}_{\gamma_h})(u_h^+ - u_h^-) \tag{2.6}$$

and

$$C(u_h, \mathbf{n}_{\gamma_h}) = \frac{1}{2} \max \left\{ \left| \frac{\partial}{\partial u} \mathbf{f}(\bar{u}_{T_h}) \cdot \mathbf{n}_{\gamma_h} \right|, \left| \frac{\partial}{\partial u} \mathbf{f}(\bar{u}_{T_h'}) \cdot \mathbf{n}_{\gamma_h} \right| \right\} \tag{2.7}$$

where $\bar{u}_{T_h}$ and $\bar{u}_{T_h'}$ are the means of the numerical solution of elements T_h and T_h' sharing the same edge γ_h.

For the numerical fluxes $\hat{\mathbf{q}}_h$ and $\hat{u}_h$, the local flux formulae proposed in [12] are used, which gives rise to what is known as the local discontinuous Galerkin (LDG) method, and allows the

variable $\mathbf{q}_h$ to be eliminated locally within each element. The local fluxes are defined as follows:

$$\hat{u}_h = u_h^- \tag{2.8}$$

$$\hat{\mathbf{q}}_h = \mathbf{q}_h^+ \tag{2.9}$$

where $(u_h^+, \mathbf{q}_h^+)$ (respectively, $(u_h^-, \mathbf{q}_h^-)$) are the traces of $(u_h, \mathbf{q}_h)$ on γ_h from the interior (respectively, the exterior) of element T_h. That is, we are taking the exterior and interior limits for the numerical fluxes of u_h and $\mathbf{q}_h$. Of course, the other pair — interior limits of u_h and exterior limits of $\mathbf{q}_h$ — could have also been taken. To eliminate the auxiliary variable, we introduce a linear operator $\mathbf{L} : X_h^p \to Y_h^p$ such that $\forall w_h \in X_h^p$, $\mathbf{L}(w_h) \in Y_h^p$ is the solution to

$$\int_{T_h} \mathbf{L}(w_h) \cdot \mathbf{r}_h = -\int_{T_h} w_h \nabla \cdot \mathbf{r}_h + \sum_{\gamma_h \in \mathcal{E}(T_h)} \int_{\gamma_h} \hat{w}_h \mathbf{r}_h \cdot \mathbf{n}_{\gamma_h}, \quad \forall \mathbf{r}_h \in Y_h^p. \tag{2.10}$$

It thus follows from (2.5) that $\mathbf{q}_h = \mathbf{L}(w_h)$, and $\hat{\mathbf{q}}_h = \hat{\mathbf{L}}(w_h)$. Hence the weak formulation from (2.5) can be rewritten in terms of the solution u_h only:

$$\begin{aligned} m\left(\frac{\partial u_h}{\partial t}, v_h\right) &= \sum_{T_h \in \mathcal{T}_h} \int_{T_h} \mathbf{f}(u_h) \cdot \nabla v_h \\ &- \sum_{\gamma_h \in \mathcal{E}(T_h)} \int_{\gamma_h} \hat{f}(u_h, \mathbf{n}_{\gamma_h}) v_h - \mu a(u_h, v_h), \quad \forall v_h \in X_h^p. \end{aligned} \tag{2.11}$$

$m(w, v)$ and $a(w, v)$ are two bilinear forms and are defined as

$$m(w, v) = \sum_{T_h \in \mathcal{T}_h} \int_{T_h} wv, \tag{2.12}$$

$$a(w, v) = \sum_{T_h \in \mathcal{T}_h} \int_{T_h} \mathbf{L}(w) \cdot \nabla v - \sum_{\gamma_h \in \mathcal{E}(T_h)} \int_{\gamma_h} \hat{\mathbf{L}}(w) \cdot \mathbf{n} v. \tag{2.13}$$

Note the weak form in (2.11) is defined over the whole domain Ω. It remains to address the time discretization.

2.2 The RK Time Discretization

To begin, we define the residual r as

$$r(w_h, v_h; \mu) = \sum_{T_h \in \mathcal{T}_h} \mathbf{f}(w_h) \cdot \nabla v_h - \sum_{\gamma_h \in \mathcal{E}(\mathcal{T}_h)} \int_{\gamma_h} \hat{f}(w_h, \mathbf{n}_{\gamma_h}) v_h - \mu a(w_h, v_h), \quad \forall v_h \in X_h^p. \tag{2.14}$$

The weak formulation (2.11) can thus be written as

$$m\left(\frac{\partial u_h}{\partial t}, v_h\right) = r\left(u_h(\mu, t), v_h; \mu\right), \quad \forall v_h \in X_h^p, \quad \text{in}(0, T]. \tag{2.15}$$

We consider the fourth-order accurate explicit Runge-Kutta scheme for time integration. We use a constant timestep Δt and discretize the time $t_k = k\Delta t,\ 0 < t_k \leq T$. The problem can be restated as: find $u_h(\mu, t_k) \in X_h^p, 1 \leq k \leq K$ such that $\forall v_h \in X_h^p$,

$$\begin{aligned} m(u_h(\mu, t_k), v_h) = m(u_h(\mu, t_{k-1}), v_h) \quad &+ \quad \frac{\Delta t}{6}\Big(r(u_h(\mu, t_{k-1}), v_h; \mu) \\ &+ \quad 2r\big(u_h(\mu, t_{k-1}) + \frac{\Delta t}{2} u_{h,1}^{k-1}, v_h; \mu\big) \\ &+ \quad 2r\big(u_h(\mu, t_{k-1}) + \frac{\Delta t}{2} u_{h,2}^{k-1}, v_h; \mu\big) \\ &+ \quad r(u_h(\mu, t_{k-1}) + \Delta t u_{h,3}^{k-1}, v_h; \mu)\Big), \end{aligned} \tag{2.16}$$

where the intermediate solutions of the field variables — $u_{h,1}^{k-1},\ u_{h,2}^{k-1},\ u_{h,3}^{k-1}$— are computed as,

$$\begin{aligned} m(u_{h,1}^{k-1}, v_h) &= r(u_h(\mu, t_{k-1}), v_h; \mu), && \forall v_h \in X_h^p \\ m(u_{h,2}^{k-1}, v_h) &= r\big(u_h(\mu, t_{k-1}) + \frac{\Delta t}{2} u_{h,1}^{k-1}, v_h; \mu\big), && \forall v_h \in X_h^p \\ m(u_{h,3}^{k-1}, v_h) &= r\big(u_h(\mu, t_{k-1}) + \frac{\Delta t}{2} u_{h,2}^{k-1}, v_h; \mu\big), && \forall v_h \in X_h^p\ . \end{aligned} \tag{2.17}$$

Note that, the initial value used for time integration is $u_h(\mu, t_0) = u_{h0}(x)$, which is the L^2 projection of $u_0(x)$ on the DG discretized space X_h^p.

Chapter 3

Reduced-Basis Methodology

In this chapter, we describe the reduced-basis methodology used to solve the nonlinear convection-diffusion problems defined in Section 1.2. The method first applies the proper orthogonal decomposition (POD) procedure to build a reduced-order basis for the field variables. For the parameter-dependent non-linear terms that arise in the PDE, it relies on the empirical interpolation procedure developed in [5, 17] to provide inexpensive coefficient-function approximation and allow efficient offline-online computational decompositions. We then discuss the reduced-basis formulation, which is based on the coefficient-function approximation for the *non-linear functions*. We will also briefly introduce another simpler formulation, which is based on the coefficient-function approximation for the *residual vector*. Asymptotic *a posterior* error estimators are then developed to quantify the accuracy of the models.

3.1 POD Procedure

We apply the POD procedure to generate basis functions for the field variables $\{\phi_n(x), 1 \leq n \leq N\}$ from a set of linearly independent "snapshots" $\{U_j(x) \equiv u_h(x;\tilde{\mu}_j), \tilde{\mu}_j \in \tilde{\mathcal{D}}, 1 \leq j \leq P\}$; here $u_h(x;\tilde{\mu}_j), 1 \leq j \leq P$, are discontinuous Galerkin solutions at different parameter-time values $\tilde{\mu}_j$; recall that $\tilde{\mu}_j$ is defined in section 1.4, as a parameter-time variable $\tilde{\mu} \equiv (\mu, t_k) \in \tilde{\mathcal{D}}$. Often, a large number of snapshots P will be chosen to describe the behavior of the system as comprehensive as possible; hence, the associated computational cost can be expensive. Given the set of snapshots, a

two-point spatial correlation function can be defined as

$$\mathcal{K}(x,x') = \frac{1}{P}\sum_{j=1}^{P} U_j(x)U_j(x') \ , \tag{3.1}$$

which accepts the following spectral decomposition

$$\mathcal{K}(x,x') = \sum_{j=1}^{P} \lambda_j \phi_j(x)\phi_j(x') \ . \tag{3.2}$$

Here the set of basis functions $\phi_j, 1 \leq j \leq P$, are orthonormal (i.e., $(\phi_i, \phi_j) = \delta_{ij}$) and ordered in such a manner that the associated eigenvalues

$$\lambda_j = \frac{1}{P}\sum_{l=1}^{P} \phi_j(x), U_l(x) \tag{3.3}$$

satisfy $\lambda_j \geq \lambda_{j+1}$.

For a given $N \leq P$, the POD procedure determines $\phi_n, 1 \leq n \leq N$, so as to maximize the captured energy

$$E_N = \sum_{n=1}^{N}\left(\frac{1}{P}\sum_{l=1}^{P}\phi_n(x), U_l(x)\right) = \sum_{n=1}^{N}\lambda_n \ . \tag{3.4}$$

The first few basis functions thus represent the main energy-containing structures in the snapshots, with their relative importance quantified by λ_k. Typically, the number of basis functions needed $N(\ll P)$ is chosen as the smallest integer satisfying $\sum_{n=1}^{N}\lambda_n / \sum_{j=1}^{P}\lambda_j \geq 0.99$. It can be shown that maximizing E_N amounts to solve the eigenfunction equation

$$(\mathcal{K}(x,x'), \phi(x')) = \lambda\phi(x) \tag{3.5}$$

for the first N eigenfunctions.

The method of snapshots [40] expresses the empirical eigenfunctions $\phi(x)$ as a linear combination of the snapshots

$$\phi(x) = \sum_{l=1}^{P} a_l U_l(x) \ . \tag{3.6}$$

Inserting this representation and (3.1) into (3.5), we immediately obtain

$$Ca = \lambda a \ , \tag{3.7}$$

where C is given by $C_{ij} = \frac{1}{P}\left(U_i(x), U_j(x)\right), 1 \leq i,j \leq K$. The eigenproblem (3.7) can then be solved for the eigenvalues and eigenvectors from which the POD basis functions $\phi_n(x), 1 \leq n \leq N$ are constructed by appealing to (3.6).

We denote by Φ_N^u the approximation space spanned by these basis functions, i.e., $\Phi_N^u = \text{span}\{\phi_1(x), \ldots, \phi_N(x)\}$. A reduced-order model for the field variables might be derived through a Galerkin projection onto this approximation space as described below.

3.2 Galerkin Approximation

Galerkin approximation of the non-linear terms refers to applying a standard Galerkin projection method and evaluating the non-linear terms of the PDEs from the reduced-basis of the field variables already established.

Applying a Galerkin approximation to our equation (2.15), using the associated reduced-basis model would give: find $u_N(\mu, t) \in \Phi_N^u$ such that

$$m(\dot{u}_N(\mu,t), v_N) = r(u_N(\mu,t), v_N; \mu), \quad \forall v_N \in \Phi_N^u, \text{ in } (0,T] \ . \tag{3.8}$$

where for any $w_N \in \Phi_N^u$, $r(w_N, v_N; \mu)$ is defined similarly as in (2.14),

$$r(w_N, v_N; \mu) = \sum_{T_h \in \mathcal{T}_h} \int_{T_h} \mathbf{f}(w_N) \cdot \nabla v_N - \sum_{\gamma_h \in \mathcal{E}(T_h)} \int_{\gamma_h} \hat{f}(w_N, \mathbf{n}_{\gamma_h}) v_N - \mu a(w_N, v_N), \quad \forall v_N \in \Phi_N^u. \tag{3.9}$$

and the numerical flux function $\hat{f}$ is defined in (2.6).

Observe that if the function $\mathbf{f}$ consists of low order polynomial functions, we could substitute $w_N = \sum_{j=1}^{N} w_{N,j}\phi_j$ into $\mathbf{f}(w_N) = (f_1(w_N), \ldots, f_d(w_N))$ and $\hat{f}(w_N, \mathbf{n})$, and easily expand them as the summations of products of the coefficients $w_{N,j}$ and basis functions ϕ_j [42, 20]; the evaluation of the residual $r(w_N, v_N; \mu)$ would then be inexpensive and readily implemented by an online-offline procedure.

Unfortunately, this strategy does not work for high-order polynomials or non-polynomial nonlinear-

ities: $r(w_N, v_N; \mu)$ can only be evaluated by explicitly constructing $w_N = \sum_{j=1}^{N} w_{N,j}\phi_j$, $\mathbf{f}(w_N)$, and $\hat{f}(w_N, \mathbf{n})$ in the *online* stage; the operation count for the online stage will therefore scale as some power of $\mathcal{N}$ — the dimension of the underlying finite element approximation space. Due to this $O(\mathcal{N})$ dependence, it is no longer ingenuous to interpret (3.8) as a reduced-order model since the resulting computational advantage relative to classical approaches using advanced iterative techniques may only be modest. Hence, the nonlinear problems raised here require a special treatment such that the incurred computational cost depends only on the dimension of reduced-basis approximation space, but *not* on $\mathcal{N}$. Towards this end, we develop a collateral reduced-basis expansion for the nonlinear terms using the empirical interpolation procedure [5, 17] reviewed below.

3.3 Empirical Interpolation Procedure

For a general parameter-dependent nonlinear function $g(w_h(x); x; \tilde{\mu})$ with $w_h \in X_h^p$, the idea here is to construct an *inexpensive* approximation $g_M^{w_h}(x; \tilde{\mu})$ to $g(w_h(x); x; \tilde{\mu})$ via an approximation space $\Psi_M^g = \text{span}\{\psi_m(x), 1 \le m \le M\}$ and associated set of interpolation points $T_M^g = \{z_1, \ldots, z_M\}$. In particular, $g_M^{w_h}(x; \tilde{\mu}) \in \Psi_M^g$ — which is known as the coefficient-function approximation [5, 17] to $g(w_h(x); x; \tilde{\mu})$ — is given by

$$g_M^{w_h}(x; \tilde{\mu}) = \sum_{m=1}^{M} \beta_m(\tilde{\mu})\psi_m(x), \tag{3.10}$$

where the coefficients $\beta_m(\tilde{\mu}), 1 \le m \le M$, satisfy

$$\sum_{m=1}^{M} \psi_m(z_i)\, \beta_m(\tilde{\mu}) = g(w_h(z_i); z_i; \tilde{\mu}), \quad 1 \le i \le M. \tag{3.11}$$

Of course, the quality of our approximation depends crucially on the basis functions and interpolation points. Here Ψ_M^g and T_M^g are determined so as to provide good approximation to $g(w_h(x), x; \tilde{\mu})$ for w_h *close* to the manifold $\mathcal{W}_h \equiv \{u_h(\tilde{\mu}) \mid \tilde{\mu} \in \tilde{\mathcal{D}}\}$. Our attention is thus directed to the manifold $\mathcal{W}_h$, *not* the entire function space X_h^p. The construction of Ψ_M^g and T_M^g are as follows.

The approximation space, $\Psi_M^g = \text{span}\{\psi_m(x), 1 \le m \le M\}$, is constructed upon the set of snapshots $\{g(u_h(\tilde{\mu}_j); \cdot; \tilde{\mu}_j), \tilde{\mu}_j \in \tilde{\mathcal{D}}, 1 \le j \le P\}$ by using the POD procedure described earlier; recall that $u_h(\tilde{\mu}_j)$ is the discontinuous Galerkin solution at $\tilde{\mu}_j$. Hence, although the coefficient-function approximation $g_M^{w_h}(x; \tilde{\mu})$ is defined for general $w_h \in X_h^p$, we expect good approximation

only for w_h close to the manifold $\mathcal{W}_h$ on which Ψ_M^g is constructed.

Once the basis set $\psi_m(x), 1 \leq m \leq M$, are available, the set of interpolation points, $T_M^g = \{z_1, \ldots, z_M\}$, can then be constructed. We first set $z_1 = \arg \operatorname{ess\,sup}_{x\in\Omega} |\psi_1(x)|$, $B_{11}^1 = \psi_1(z_1)$. Then for $m = 2, \ldots, M$, we solve the linear system $\sum_{j=1}^{m-1} \sigma_j^{m-1} \psi_j(z_i) = \psi_m(z_i)$, $1 \leq i \leq m-1$, and set $r_m(x) = \psi_m(x) - \sum_{j=1}^{m-1} \sigma_j^{m-1} \psi_j(x)$, $z_m = \arg \operatorname{ess\,sup}_{x\in\Omega} |r_m(x)|$, and $B_{ij}^m = \psi_j(z_i)$, $1 \leq i, j \leq m$. It can be shown that the matrix $B_{ij}^M = \psi_j(z_i)$, $1 \leq i, j \leq M$, constructed in such way is invertible [5, 17].

Theoretical and numerical aspects of the empirical interpolation have been analyzed in great detail in [5, 17]. Note however that the presented procedure slightly differs from the procedure outlined in [5, 17] in the choice of basis functions: rather than forming the basis with a greedy selection process as in [5, 17], we choose to use the POD procedure; and the orthonormalization of the basis set becomes unnecessary as our POD basis set is already orthonormal with respect to the L^2 inner product. We are now ready to incorporate this empirical interpolation into the Galerkin approximation for the efficient evaluation of the reduced-order model.

3.4 Reduced-Basis Formulation

3.4.1 Formulation I: Function Approximation

Fully Discrete Equations

To begin, we first define the necessary approximation spaces and the associated interpolation points for nonlinear terms:

- field variable u, $\Phi_N^u = \operatorname{span}\{\phi_1(x), \ldots, \phi_N(x)\}$;
- nonlinear functions f_g, $1 \leq g \leq d$, $\Psi_{M^g}^g = \operatorname{span}\{\psi_1^g, \ldots, \psi_{M^g}^g\}$, $T_{M^g}^g = \{z_1^g, \ldots, z_{M^g}^g\}$;
- nonlinear numerical flux function $\hat{f}$, $\hat{\Psi}_{\hat{M}} = \operatorname{span}\{\hat{\psi}_1, \ldots, \hat{\psi}_{\hat{M}}, \}$, $\hat{T}_{\hat{M}} = \{\hat{z}_1, \ldots, \hat{z}_{\hat{M}^i}\}$.

For simplicity, we assume that $M^g = \hat{M} = M, 1 \leq g \leq d$, throughout this section. Note that the coefficient-function approximations are defined on $\mathcal{T}_h$ for the nonlinear function $f_g(u_N), 1 \leq g \leq d,$, but on $\mathcal{E}(\mathcal{T}_h)$ for the nonlinear numerical flux function $\hat{f}$.

Next, by replacing the nonlinear terms $f_g(u_N(\mu, t)), 1 \leq g \leq d$, and $\hat{f}(u_N(\mu, t), \mathbf{n})$ with the coefficient-function approximations $f_{g,M}^{u_N,M}(x; \mu, t), 1 \leq g \leq d$, and $\hat{f}_M^{u_N,M}(x; \mu, t)$, we obtain the

reduced-basis model: given $\mu \in \mathcal{D}$, we are to evaluate

$$s_{N,M}(\mu,t) = \ell(u_{N,M}(\mu,t)), \quad \text{in } (0,T], \tag{3.12}$$

where $u_{N,M} \in \Phi_N^u$ is solved by

$$m(\dot{u}_{N,M}(\mu,t), v_N) = \tilde{r}(u_{N,M}(\mu,t), v_N; \mu), \quad \forall v_N \in \Phi_N^u, \text{ in } (0,T] \ . \tag{3.13}$$

For the reduced-basis model, the residual vector $\tilde{r}(w_N, v_N; \mu)$ is defined as

$$\begin{aligned}\tilde{r}(w_N, v_N; \mu) = \sum_{T_h \in \mathcal{T}_h} \sum_{g=1}^{d} \int_{T_h} f_{g,M}^{w_N}(x) \frac{\partial v_N}{\partial x_g} \\ - \sum_{\gamma_h \in \mathcal{E}(\mathcal{T}_h)} \int_{\gamma_h} \hat{f}_M^{w_N}(x) v_N - \mu a(w_N, v_N), \quad \forall v_N \in \Phi_N^u \ ,\end{aligned} \tag{3.14}$$

where $f_{g,M}^{w_N}, 1 \le g \le d$, and $\hat{f}_M^{w_N}$ are computed by

$$\begin{aligned} f_{g,M}^{w_N}(x) &= \sum_{m=1}^{M} \beta_m^g \psi_m^g(x), \quad \sum_{m=1}^{M} \psi_m^g(z_j^g)\beta_m^g = f_g(w_N(z_j^g), \quad 1 \le g \le d, \ 1 \le j \le M \\ \hat{f}_M^{w_N}(x) &= \sum_{m=1}^{M} \hat{\beta}_m \hat{\psi}_m(x), \quad \sum_{m=1}^{M} \hat{\psi}_m(\hat{z}_j)\hat{\beta}_m = \hat{f}(w_N(\hat{z}_j), \mathbf{n}(\hat{z}_j)), \quad 1 \le j \le M. \end{aligned} \tag{3.15}$$

Again, using the fourth-order accurate explicit Runge-Kutta scheme, we integrate the reduced-basis system (3.13) in time and obtain $u_{N,M}(\mu, t_k), k = 1, \ldots, K$, from

$$\begin{aligned} m(u_{N,M}(\mu,t_k), v_N) = m(u_{N,M}(\mu,t_{k-1}), v_N) + \frac{\Delta t}{6}\Big(\tilde{r}(u_{N,M}(\mu,t_{k-1}), v_N; \mu) \\ + 2\tilde{r}(u_{N,M}(\mu,t_{k-1}) + \frac{\Delta t}{2} u_{N,M,1}^{k-1}, v_N; \mu) + 2\tilde{r}(u_{N,M}(\mu,t_{k-1}) + \frac{\Delta t}{2} u_{N,M,2}^{k-1}, v_N; \mu) \\ + \tilde{r}(u_{N,M}(\mu,t_{k-1}) + \Delta t u_{N,M,3}^{k-1}, v_N; \mu)\Big), \quad \forall v_N \in \Phi_N^u \ , \end{aligned} \tag{3.16}$$

where intermediate solutions of the field variables — $u^{k-1}_{N,M,1}, u^{k-1}_{N,M,2}$, and $u^{k-1}_{N,M,3}$ — are solved from

$$\begin{aligned} m(u^{k-1}_{N,M,1}, v_N) &= \tilde{r}(u_{N,M}(\mu, t_{k-1}), v_N; \mu), && \forall v_N \in \Phi^u_N \\ m(u^{k-1}_{N,M,2}, v_N) &= \tilde{r}(u_{N,M}(\mu, t_{k-1}) + \frac{\Delta t}{2} u^{k-1}_{N,M,1}, v_N; \mu), && \forall v_N \in \Phi^u_N \\ m(u^{k-1}_{N,M,3}, v_N) &= \tilde{r}(u_{N,M}(\mu, t_{k-1}) + \frac{\Delta t}{2} u^{k-1}_{N,M,2}, v_N; \mu), && \forall v_N \in \Phi^u_N \ . \end{aligned} \tag{3.17}$$

The RB output at a discrete time instance will then be calculated as

$$s_{N,M}(\mu, t_k) = \ell(u_{N,M}(\mu, t_k)), \quad 1 \leq k \leq K \ . \tag{3.18}$$

In what follows, we develop a computational procedure which allows to solve the linear system in (3.16) and evaluate our RB output efficiently.

Offline-Online Procedure

We first need to express the field variable as a linear combination of the basis functions

$$u_{N,M}(\mu, t_k) = \sum_{j=1}^{N} \alpha_j(\mu, t_k)\phi_j \ . \tag{3.19}$$

Substituting this representation into (3.16) and using the same bases for v_N, i.e. $v_N = \phi_i, 1 \leq i \leq N$, we have the following linear system for the coefficients $\alpha_j(\mu, t_k), 1 \leq j \leq N$,

$$\begin{aligned} \sum_{j=1}^{N} m(\phi_j, \phi_i)\alpha_j(\mu, t_k) = \sum_{j=1}^{N} m(\phi_j, \phi_i)\alpha_j(\mu, t_{k-1}) + \frac{\Delta t}{6}\Big(\tilde{r}(u_{N,M}(\mu, t_{k-1}), \phi_i; \mu) \\ + 2\tilde{r}\big(u_{N,M}(\mu, t_{k-1}) + \frac{\Delta t}{2} u^{k-1}_{N,M,1}, \phi_i; \mu\big) + 2\tilde{r}\big(u_{N,M}(\mu, t_{k-1}) + \frac{\Delta t}{2} u^{k-1}_{N,M,2}, \phi_i; \mu\big) \\ + \tilde{r}(u_{N,M}(\mu, t_{k-1}) + \Delta t u^{k-1}_{N,M,3}, \phi_i; \mu)\Big), \quad i = 1, \ldots, N. \end{aligned} \tag{3.20}$$

The initial coefficient $\alpha_j(\mu, t_0)$ needs to satisfy

$$\alpha_j(\mu, t_0) = (\phi_j, u_h(\mu, t_0)) \tag{3.21}$$

Here $u^{k-1}_{N,M,1} = \sum_{j=1}^{N} \alpha^{k-1}_{1,j}\phi_j$, $u^{k-1}_{N,M,2} = \sum_{j=1}^{N} \alpha^{k-1}_{2,j}\phi_j$, and $u^{k-1}_{N,M,3} = \sum_{j=1}^{N} \alpha^{k-1}_{3,j}\phi_j$, and the coefficients $\alpha^{k-1}_{1,j}$, $\alpha^{k-1}_{2,j}$, $\alpha^{k-1}_{3,j}$,$1 \le j \le N$, need to satisfy

$$\begin{aligned}
&\sum_{j=1}^{N} m(\phi_j,\phi_i)\alpha^{k-1}_{1,j} = \tilde{r}(u_{N,M}(\mu,t_{k-1}),\phi_i;\mu), && 1 \le i \le N \\
&\sum_{j=1}^{N} m(\phi_j,\phi_i)\alpha^{k-1}_{2,j} = \tilde{r}\Big(u_{N,M}(\mu,t_{k-1}) + \frac{\Delta t}{2}u^{k-1}_{N,M,1},\phi_i;\mu\Big), && 1 \le i \le N \\
&\sum_{j=1}^{N} m(\phi_j,\phi_i)\alpha^{k-1}_{3,j} = \tilde{r}\Big(u_{N,M}(\mu,t_{k-1}) + \frac{\Delta t}{2}u^{k-1}_{N,M,2},\phi_i;\mu\Big), && 1 \le i \le N\ .
\end{aligned} \tag{3.22}$$

For any $w_N = \sum_{j=1}^{N} w_{N,j}\phi_j$ inΨ^u_N, the reduced-basis residual can now be evaluated as

$$\begin{aligned}
\tilde{r}(w_N,\phi_i;\mu) = \sum_{g=1}^{d}\sum_{m=1}^{M}\beta^g_m \sum_{T_h\in\mathcal{T}_h}\int_{T_h}\psi^g_m(x)\frac{\partial\phi_i}{\partial x_g} \\
- \sum_{m=1}^{M}\hat{\beta}_m \sum_{\gamma_h\in\mathcal{E}(\mathcal{T}_h)}\int_{\gamma_h}\hat{\psi}_m(x)\phi_i - \mu\sum_{j=1}^{N} w_{N,j}a(\phi_j,\phi_i),
\end{aligned} \tag{3.23}$$

where the coefficients $\beta^g_m, \hat{\beta}_m, 1 \le f \le d, 1 \le g \le M$, are calculated from

$$\begin{aligned}
&\sum_{m=1}^{M}\psi^g_m(z^g_i)\beta^p_m = f_g\Big(\sum_{j=1}^{N} w_{N,j}\phi_j(z^g_i)\Big), && 1 \le g \le d, 1 \le i \le M \\
&\sum_{m=1}^{M}\hat{\psi}_m(\hat{z}_i)\hat{\beta}_m = \hat{f}\Big(\sum_{j=1}^{N} w_{N,j}\phi_j(\hat{z}_i),\mathbf{n}(\hat{z}_i)\Big), && 1 \le i \le M\ .
\end{aligned} \tag{3.24}$$

We have now successfully decomposed the residual $\tilde{r}(w_N,\phi_i;\mu)$ into a summation of products of parameter-dependent coefficients and parameter-independent quantities, the approximation procedure thus admits an offline/online computation decomposition [26, 35, 4, 20, 28]. For practical implementation purposes, we rewrite the equations (3.20) – (3.24) in the form of vector-matrix products. Let's first introduce the following parameter-independent matrices and vectors.

$$\begin{aligned}
&A^1_{ij} = m(\phi_j,\phi_i), A^2_{ij} = a(\phi_j,\phi_i), L_j = \ell(\phi_j), \alpha_{0j} = (u_{h0},\phi_j), && 1 \le i,j \le N \\
&B^g_{ij} = \psi^g_j(z^g_i),\ \hat{B}_{ij} = \hat{\psi}_j(\hat{z}_i), && 1 \le g \le d, 1 \le i,j \le M \\
&C^g_{ij} = \textstyle\sum_{T_h\in\mathcal{T}_h}\int_{T_h}\psi^g_j\frac{\partial\phi_i}{\partial x_g},\ \hat{C}_{ij} = \sum_{\gamma_h\in\mathcal{E}(\mathcal{T}_h)}\int_{\gamma_h}\hat{\psi}_j\phi_i, && 1 \le g \le d, 1 \le i \le N, 1 \le j \le M \\
&D^g_{ij} = \phi_j(z^g_i),\ \hat{D}_{ij} = \phi_j(\hat{z}_i), \hat{n}_i = \mathbf{n}(\hat{z}_i), && 1 \le g \le d, 1 \le j \le N, 1 \le i \le M.
\end{aligned}$$

It thus follows that the reduced-basis output can be calculated as

$$s_{N,M}(\mu, t_k) = L^T \alpha(\mu, t_k), \quad k = 1, \ldots, K \ , \tag{3.25}$$

where $\alpha(\mu, t_k) \in \mathbb{R}^N$ is the new unknown of interest in our reduced-basis approximation model, instead of $u(\mu, t_k) \in \mathbb{R}^{\mathcal{N}}$, and is the solution of

$$\begin{aligned}\alpha(\mu, t_k) = \alpha(\mu, t_{k-1}) + \frac{\Delta t}{6}\Big(&\tilde{R}(\alpha(\mu, t_{k-1})) + 2\tilde{R}\big(\alpha(\mu, t_{k-1}) + \frac{\Delta t}{2}\alpha_1^{k-1}\big) \\ &+ 2\tilde{R}\big(\alpha(\mu, t_{k-1}) + \frac{\Delta t}{2}\alpha_2^{k-1}\big) + \tilde{R}\big(\alpha(\mu, t_{k-1}) + \Delta t\alpha_3^{k-1}\big)\Big), \quad k = 1, \ldots, K \ .\end{aligned} \tag{3.26}$$

From (3.22), the coefficients α_1^{k-1},α_2^{k-1}, and α_3^{k-1} can be calculated from

$$\begin{aligned}\alpha_1^{k-1} &= \tilde{R}(\alpha(\mu, t_{k-1})) \\ \alpha_2^{k-1} &= \tilde{R}\Big(\alpha(\mu, t_{k-1}) + \frac{\Delta t}{2}\alpha_1^{k-1}\Big) \\ \alpha_3^{k-1} &= \tilde{R}\Big(\alpha(\mu, t_{k-1}) + \frac{\Delta t}{2}\alpha_2^{k-1}\Big) \ ,\end{aligned} \tag{3.27}$$

and from (3.23), for any $\sigma \in \mathbb{R}^N$, the reduced-basis residual vector can be calculated as

$$\tilde{R}(\sigma) = E^1 f_1\left(D^1\sigma\right) + E^2 f_2\left(D^2\sigma\right) + \hat{E}\hat{f}\big(\hat{D}\sigma, \hat{n}\big) - \mu E\sigma \ , \tag{3.28}$$

where $E^1 = (A^1)^{-1}C^1\left(B^1\right)^{-1}$, $E^2 = (A^1)^{-1}C^2\left(B^2\right)^{-1}$, $\hat{E} = (A^1)^{-1}\hat{C}(\hat{B})^{-1}$, and $E = (A^1)^{-1}A^2$.

Finally, the offline/online procedure for the efficient evaluation of $s_{N,M}(\mu, t_k)$ is implemented as follows:

— In the offline stage, (performed *once*)

- First, solve for the DG solutions of the field variable, which consist the snapshots set $\{u_h(x; \tilde{\mu}_p), \tilde{\mu}_p \in \tilde{\mathcal{D}}, 1 \le p \le P\}$
- Next, apply the POD procedure to construct the approximation space of the field variable Φ_N^u, and the approximation space of the nonlinear terms $\Psi_M^g, \hat{\Psi}_M, 1 \le g \le d$.
- Then use the empirical interpolation procedure to obtain the sets of interpolation points $T_M^g, \hat{T}_M, 1 \le g \le d$, for the nonlinear terms.

- Finally form and *store* the parameter-independent quantities $D^g, \hat{D}, E, E^g, \hat{E}, \hat{n}$, and $\alpha_0, 1 \leq g \leq d$.

— In the online stage (performed *many* times), we simply perform the sum (3.26) to obtain $\alpha(\mu, t_k) \in \mathbb{R}^N$, and evaluate $s_{N,M}(\mu, t_k)$ from (3.25).

With this decomposition, the cost of our reduced-basis approach is determined by the operation count for the online stage: computing $\hat{R}(\sigma)$ takes $O(6MN + N^2)$ function evaluations; performing the sum in (3.26) requires four evaluations of $\hat{R}(\sigma)$; moreover, the output evaluation in (3.25) takes $O(2N)$ operations. In summary, the total operation count is $O(4K(6MN + N^2))$. Not surprisingly, the complexity of online stage is independent of $\mathcal{N}$. To expect significant savings relative to the DG approximation $s_h(\mu, t_k)$, it is required that $M, N \ll \mathcal{N}$.

3.4.2 Formulation II: Residual Approximation

Another reduced-basis formulation, which is simpler in implementation, but less stable than the previous formulation, will be briefly introduced in this section. This second formulation aims to form a reduced-basis model via the coefficient-function approximation for the residual-vector directly, instead of for the nonlinear functions in the first formulation.

Fully Discrete Equations

To begin, we write the Galerkin approximation (3.8) in the following form

$$\Phi^T \mathbf{M} \frac{\partial u_N(\mu, t)}{\partial t} = \Phi^T R(u_N(\mu, t); \mu), \quad \text{in } (0, T] \,. \tag{3.29}$$

Here $\Phi = [\phi_1, \ldots, \phi_N]$ is the matrix of N basis vectors; $\mathbf{M}$ is the mass matrix and is calculated as $\mathbf{M}_{ij} = m(\varphi_j, \varphi_i), 1 \leq i, j \leq \mathcal{N}$; and the residual vector $R(w; \mu), \forall w \in \mathbb{R}^{\mathcal{N}}$ is calculated as

$$\begin{aligned} R(w;\mu) &= \sum_{g=1}^{d} \sum_{T_h \in \mathcal{T}_h} \int_{T_h} f_g\Big(\sum_{j=1}^{\mathcal{N}} \varphi_j(x) w_j\Big) \sum_{i=1}^{\mathcal{N}} \frac{\partial \varphi_i(x)}{\partial x_g} v_i \\ &- \sum_{\gamma_h \in \mathcal{E}(\mathcal{T}_h)} \int_{\gamma_h} \hat{f}\Big(\sum_{j=1}^{\mathcal{N}} \varphi_j(x) w_j, \mathbf{n}\Big) \sum_{i=1}^{\mathcal{N}} \varphi_i(x) v_i \\ &- \mu a\Big(\sum_{j=1}^{\mathcal{N}} \varphi_j(x) w_j, \sum_{i=1}^{\mathcal{N}} \varphi_i(x) v_i\Big), \quad \forall v \in \mathbb{R}^{\mathcal{N}} \,, \end{aligned} \tag{3.30}$$

where $\varphi_j(x), 1 \le j \le \mathcal{N}$, are the finite element basis functions associated with the space X_h^p. Similarly as before, besides the approximation space for the field variable, we also need an approximation space for the nonlinear terms. In this case, it is the residual function $R(w;\mu)$ in (3.30). We denote the approximation space by $\Psi_M^R = \text{span}\{\psi_1^R, \ldots, \psi_M^R\} \in \mathbb{R}^{\mathcal{N}\times N}$, and the associated set of interpolation points by $T_M^R = \{z_1^R, \ldots, z_M^R\}$; moreover, we denote the nonlinear term approximation space evaluated at the interpolation points by a square matrix, $B_{im} = \psi_m^R(z_i^R), 1 \le i, m \le M$. It then follows that our coefficient-function approximation $R_M^w(x;\mu,t)$ to $R(w(\mu,t);\mu)$ for any $w(\mu,t) \in \mathbb{R}^{\mathcal{N}}$ is given by

$$R_M^w(x;\mu,t) = \Psi\beta(\mu,t), \qquad B\beta(x;\mu,t) = b^w(\mu,t)\ , \tag{3.31}$$

where $b^w(\mu,t) \in \mathbb{R}^M$ with $b_m^w(\mu,t), 1 \le m \le M$, are the values of $R(w(\mu,t);\mu)$ evaluated at the z_m^R. By writing $u_{N,M}(\mu,t) = \Phi\alpha(\mu,t)$ and replacing $R(u_N(\mu,t);\mu)$ of (3.29) with $R_M^{u_{N,M}}(x;\mu,t)$ of (3.31), we can reach the reduced-order model: given $\mu \in \mathcal{D}$, we are to compute the output

$$s_{N,M}(\mu,t_k) = L^T\alpha(\mu,t_k), \quad \text{in} \quad 1 \le k \le K, \tag{3.32}$$

where $\alpha(\mu,t_k) \in \mathbb{R}^N$ is the solution of

$$\begin{aligned}\alpha(\mu,t_k) = \alpha(\mu,t_{k-1}) + \frac{\Delta t}{6}E\Big(&b\big(u_{NM}(\mu,t_{k-1})\big) + 2b\big(u_{NM}(\mu,t_{k-1}) + \frac{\Delta t}{2}u_{NM,1}^{k-1}\big)\\ &+2b\big(u_{NM}(\mu,t_{k-1}) + \frac{\Delta t}{2}u_{NM,2}^{k-1}\big) + b\big(u_{NM}(\mu,t_{k-1}) + \Delta t u_{NM,3}^{k-1}\big)\Big)\end{aligned} \tag{3.33}$$

here $u_{NM,1}^{k-1} = \Phi\alpha_1^{k-1}$,$u_{NM,2}^{k-1} = \Phi\alpha_2^{k-1}$, and $u_{NM,3}^{k-1} = \Phi\alpha_3^{k-1}$, and the coefficients α_1^{k-1}, α_2^{k-1}, and α_3^{k-1} are calculated from

$$\begin{aligned}\alpha_1^{k-1} &= Eb\big(u_{NM}(\mu,t_{k-1})\big),\\ \alpha_2^{k-1} &= Eb\big(u_{NM}(\mu,t_{k-1}) + \frac{\Delta t}{2}u_{NM,1}^{k-1}\big),\\ \alpha_3^{k-1} &= Eb\big(u_{NM}(\mu,t_{k-1}) + \frac{\Delta t}{2}u_{NM,2}^{k-1}\big).\end{aligned} \tag{3.34}$$

and $A = \Phi^T\mathbf{M}\Phi$, $C = \Phi^T\Psi$, $E = A^{-1}CB^{-1}$, and $L \in \mathbb{R}^N$ with $L_j = \ell(\phi_j), 1 \le j \le N$.

Offline-Online Procedure

The reduced-basis model in (3.32) – (3.34) is now ready for offline-online decomposition. Similarly to the first formulation,

— In the offline stage, (performed *once*)

- First, solve for the DG solutions of the field variable, which consist the snapshot set $\{u_h(x;\tilde{\mu}_p), \tilde{\mu}_p \in \tilde{\mathcal{D}}, 1 \leq p \leq P\}$
- Next, apply the POD procedure to construct the approximation space of the field variable Φ_N^u, and the approximation space of the nonlinear residual vector Ψ_M^R.
- Then use the empirical interpolation procedure to obtain the set of interpolation points T_M^R for the residual vector.
- Finally form and *store* the parameter-independent quantities $\Phi, \Psi,$ and E.

— In the online stage (performed *many* times), we simply perform the sum (3.33) to obtain $\alpha(\mu, t_k) \in \mathbb{R}^N$, and evaluate $s_{N,M}(\mu, t_k)$ from (3.32).

The online operation count in this formulation is $O(4K(MN + \kappa M))$ to solve for the reduced-basis coefficients $\alpha(\mu, t_k), 0 \leq k \leq K$, and $O(KN)$ to compute the output $s_{N,M}(\mu, t_k)$ at $t^k, 0 \leq k \leq K$. Note that to compute $b^{u_{N,M}}(\mu, t_k)$ means to compute the residual vector $R(\Phi\alpha(\mu, t_k); \mu)$ at the M interpolation points, which costs $O(\kappa M)$ operations; the factor κ depends on the dimensionality of the problem d and polynomial order of approximations p.

3.5 A *Posterior* Error Estimator

The reliability of very low-dimensional reduced-basis approximations of parametrized partial differential equations can only be assured by a posteriori error estimation procedures. To ensure that our RB approximation satisfies the accuracy level of interest, we hence need to develop associated a *posterior* error estimators. Following [35], we define *asymptotic* output upper and lower estimators respectively as

$$s_{N,M}^{\pm}(\mu, t_k) = s_{N,M}(\mu, t_k) \pm \Delta_{N,M}^s(\mu, t_k), \tag{3.35}$$

where $\Delta^s_{N,M}(\mu, t_k)$, the output error estimator, is given by

$$\Delta^s_{N,M}(\mu, t_k) = \frac{1}{\tau} |s_{2N,2M}(\mu, t_k) - s_{N,M}(\mu, t_k)| \tag{3.36}$$

for some $\tau \in (0, 1)$. In addition, we define the *asymptotic* error estimator for the error norm $\|u_h(\mu, t_k) - u_{N,M}(\mu, t_k)\|$

$$\Delta^u_{N,M}(\mu, t_k) = \frac{1}{\tau} \|u_{2N,2M}(\mu, t_k) - u_{N,M}(\mu, t_k)\| \tag{3.37}$$

Here $s_{2N,2M}(\mu, t_k)$ and $u_{2N,2M}(\mu, t_k)$ are the RB output and solution associated with the "twice-richer" approximation spaces $\{\Phi^u_{2N}, \Psi^{f_g}_{2M}, \Psi^{\hat{f}}_{2M}\}$ (for *function* approximation formulation), or $\{\Phi^u_{2N}, \Psi^R_{2M}\}$ (for *residual* approximation formulation). Hence, in terms of computational cost, $\Delta^s_{N,M}(\mu, t_k)$ will be four times more expensive than $s_{N,M}(\mu, t_k)$.

To measure the sharpness of our error estimators, the effectivities are introduced,

$$\eta^s_{N,M}(\mu, t_k) = \frac{\Delta^s_{N,M}(\mu, t_k)}{|s_h(\mu, t_k) - s_{N,M}(\mu, t_k)|}, \quad \eta^u_{N,M}(\mu, t_k) = \frac{\Delta^u_{N,M}(\mu, t_k)}{\|u_h(\mu, t_k) - u_{N,M}(\mu, t_k)\|} . \tag{3.38}$$

It thus follows that

$$\frac{1}{\tau}(1 - \epsilon^s) \le \eta^s_{N,M}(\mu, t_k) \le \frac{1}{\tau}(1 + \epsilon^s) , \quad \frac{1}{\tau}(1 - \epsilon^u) \le \eta^u_{N,M}(\mu, t_k) \le \frac{1}{\tau}(1 + \epsilon^u) . \tag{3.39}$$

where

$$\epsilon^s = \frac{|s_h(\mu, t_k) - s_{2N,2M}(\mu, t_k)|}{|s_h(\mu, t_k) - s_{N,M}(\mu, t_k)|} , \quad \epsilon^u = \frac{\|u_h(\mu, t_k) - u_{2N,2M}(\mu, t_k)\|}{\|u_h(\mu, t_k) - u_{N,M}(\mu, t_k)\|} . \tag{3.40}$$

Hence, under the hypothesis that $\epsilon^s \to 0$, as $N \to \infty, M \to \infty$, there exist finite integers N^* and M^* such that $\eta^s_{N,M}(\mu, t_k) \ge 1$, $\forall N \ge N^*$, $\forall M \ge M^*$. In general, our error estimator $\Delta^s_{N,M}(\mu, t_k)$ is not quite a rigorous upper bound. However, if $\epsilon^s \to 0$ very fast, we expect that the effectivity $\eta^s_{N,M}(\mu, t_k)$ shall be close to $1/\tau$. A similar argument applies for $\Delta^u_{N,M}(\mu, t_k)$.

In the following section, we will apply the the two RB approximation formulations developed so far to two problems, namely, 1D viscous Burger problem and 2D Buckley-Leverret problem. The *a posterior* error estimators described in this section will be applied to certify the results.

3.6 Numerical Examples

3.6.1 One-Dimensional Viscous Burger's Equation

The first example we present here is the one-dimensional viscous Burger's equation

$$\frac{\partial u}{\partial t} + \nabla \frac{1}{2} u^2 - \nu \nabla^2 u = 0, \quad \text{in } \Omega \times (0, 0.3] \tag{3.41}$$

with initial data $u_0(x) = 1/4 + sin(\pi(2x-1))/2$ and periodic boundary condition on boundary $\partial\Omega$. Here $\Omega \equiv]0,1[$, the viscosity ν varies in the range $\mathcal{D} \equiv [0.01, 0.1]$. The output $s(\mu, t)$ is evaluated as $s(\mu, t) = \ell(u(\mu, t))$ for $\ell(v) = \int_\Omega v$.

The purpose of this simple 1D nonlinear problem is to illustrate and compare two different reduce-basis treatment for the nonlinear term "$\frac{1}{2}u^2$", namely, Galerkin approximation and empirical interpolation procedure. As described in Section 3.2, Galerkin approximation can be used for the low order polynomial present in viscous Burger's equation. However, note that this does not apply to the numerical flux term $\hat{f}$ that arises in the RKDG method; hence, continuous Galerkin (CG) space discretization has to be used for this purpose, as there is no numerical flux term involved in this method.

In this time-dependent problem, we define the maximum relative error of solution as

$$\epsilon^u_{N,M,max,rel} = \max_{\tilde{\mu} \in \tilde{\mathcal{D}}} ||u(\tilde{\mu}) - u_{N,M}(\tilde{\mu})||_X / ||u(\tilde{\mu})||_X \tag{3.42}$$

and maximum relative output error as

$$\epsilon^s_{N,M,max,rel} = \max_{\tilde{\mu} \in \tilde{\mathcal{D}}} |s(\tilde{\mu}) - s_{N,M}(\tilde{\mu})| / |s(\tilde{\mu})| \tag{3.43}$$

In Figures 3-1 to 3-4, we present the convergence of *solution* and *output* of the two approximations, namely, Galerkin approximation and empirical interpolation approximation.

From these four figures, it is observed that the errors in both solution and output converge as the dimension of the reduced-basis model increases. Eventually, the empirical interpolation approximation method (with sufficient interpolation points, i.e. larger M) is able to achieve a comparable accuracy level as the Galerkin approximation method[1].

[1]Note that the convergence of Galerkin approximation only depends on N.

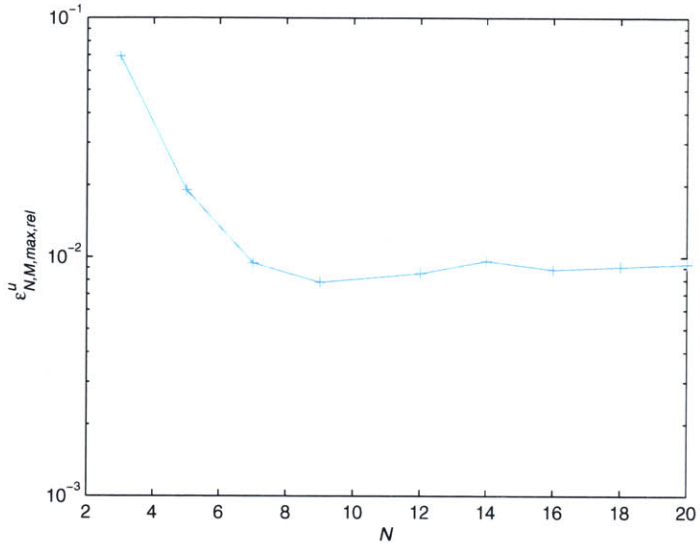

Figure 3-1: Convergence of *solution* of the reduced-basis Galerkin approximation for One-Dimensional Burger's equation

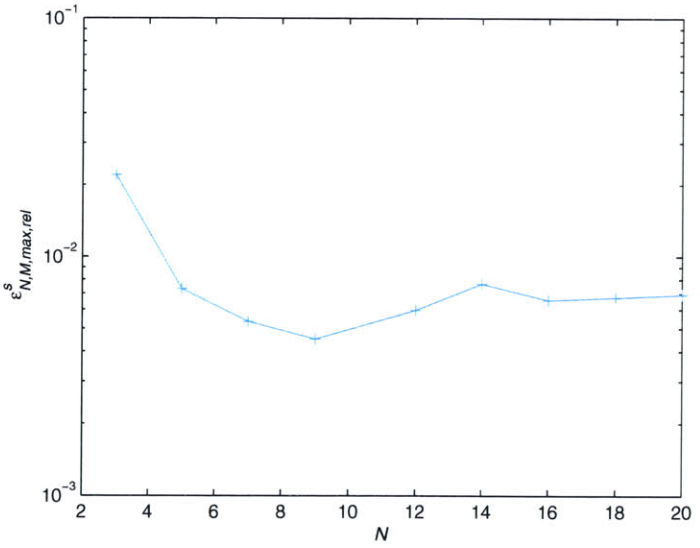

Figure 3-2: Convergence of *output* of the reduced-basis Galerkin approximation for One-Dimensional Burger's equation

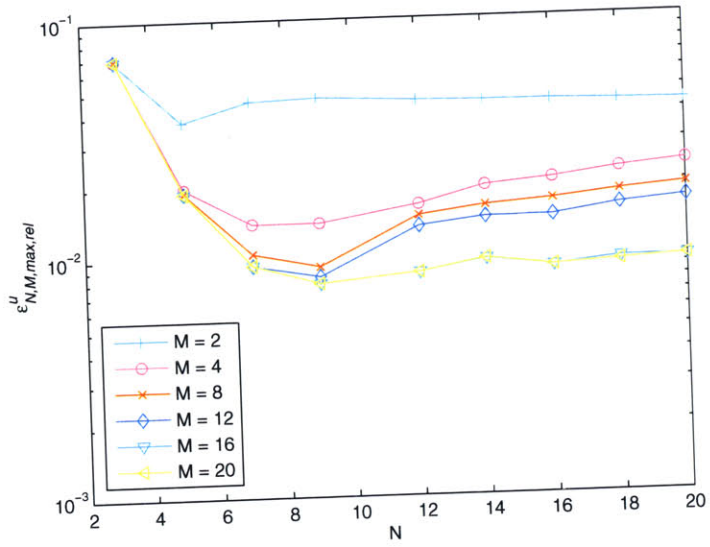

Figure 3-3: Convergence of *solution* of the reduced-basis empirical interpolation approximation for One-Dimensional Burger's equation

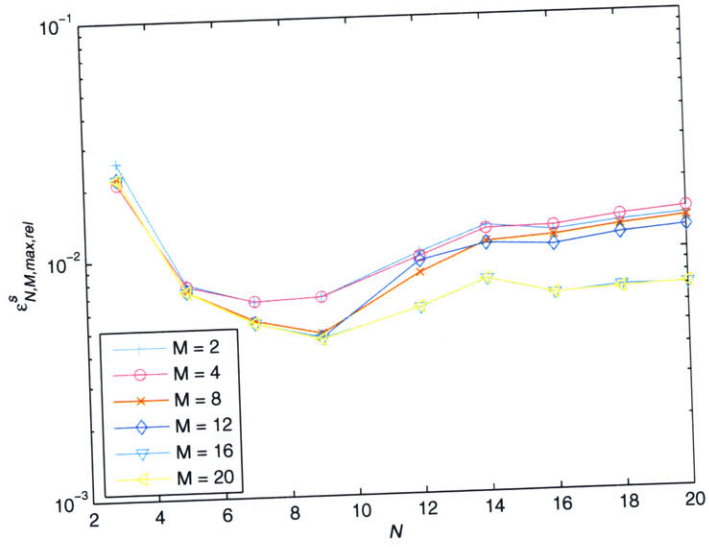

Figure 3-4: Convergence of *output* of the reduced-basis empirical interpolation approximation output for One-Dimensional Burger's equation

Table 3.1: Effectivites of Galerkin approximation for One-Dimensional viscous Burger's equation

N	$\Delta^s_{N,2N}$	$\eta^s_{N,M}$	$\Delta^u_{N,2N}$	$\eta^u_{N,M}$
2	1.8835×10^{-1}	2.0353	2.3381×10^{-1}	1.9006
4	2.2233×10^{-2}	4.0924	3.0029×10^{-2}	1.8342
7	5.3567×10^{-3}	1.2784	9.4860×10^{-3}	1.2737
10	6.2330×10^{-3}	1.6392	9.4688×10^{-3}	1.4006

Table 3.2: Effectivites of empirical interpolation approximation for One-Dimensional viscous Burger's equation

N	$\Delta^s_{N,2N}$	$\eta^s_{N,M}$	$\Delta^u_{N,2N}$	$\eta^u_{N,M}$
2	1.8862×10^{-1}	1.9991	2.3378×10^{-1}	1.8990
4	2.2249×10^{-2}	3.8922	3.0193×10^{-2}	1.8324
7	5.3516×10^{-3}	1.2886	9.4548×10^{-3}	1.2737
10	6.9435×10^{-3}	1.6399	9.4026×10^{-3}	1.4011

To verify that both our RB approximations satisfy the accuracy level of interest, we use the *a posteriori* error estimators introduced in Section 3.5, and $\tau = 0.5$. The effectivities are presented in Table 3.1 and 3.2, and they are of order $O(1)$ as $\epsilon \to 0$.

The empirical interpolation approximation method has shown as good performance as the direct Galerkin approximation method. Moreover, the online stage computational time cost (normalized with respect to CG approach) tabulated in Table 3.3 reveals that the empirical interpolation approximation is more efficient than Galerkin approximation, as it provides special treatment and construct reduced-basis for the nonlinear terms as well.

3.6.2 Two-Dimensional Buckley-Leverett Equation

Problem Description

Our second example is the two-dimensional Buckley-Leverett equation

$$\frac{\partial u}{\partial t} + \nabla \cdot \mathbf{f}(u) - \nu \nabla^2 u = 0, \quad \text{in } \Omega \times (0, 0.5] \tag{3.44}$$

with the initial data $u_0(x) = e^{-(x^2+y^2)/0.025}$ and homogeneous Dirichlet boundary condition on the boundary $\partial\Omega$. Here $\Omega \equiv]-1.25, 1.25[\times]-1.25, 1.25[$, the viscosity ν varies in the range

Table 3.3: Online computational time for One-Dimensional viscous Burger's equation

N	*Galerkin Approx.*	N	M	*Empirical Interp. Approx.*	*CG*
2	8.5498×10^{-3}	2	4	4.1173×10^{-3}	1
4	8.6896×10^{-3}	4	8	4.2184×10^{-3}	1
8	9.7093×10^{-3}	8	16	4.4452×10^{-3}	1
16	1.0625×10^{-2}	16	32	5.0195×10^{-3}	1
20	1.0876×10^{-2}	20	40	5.0564×10^{-3}	1

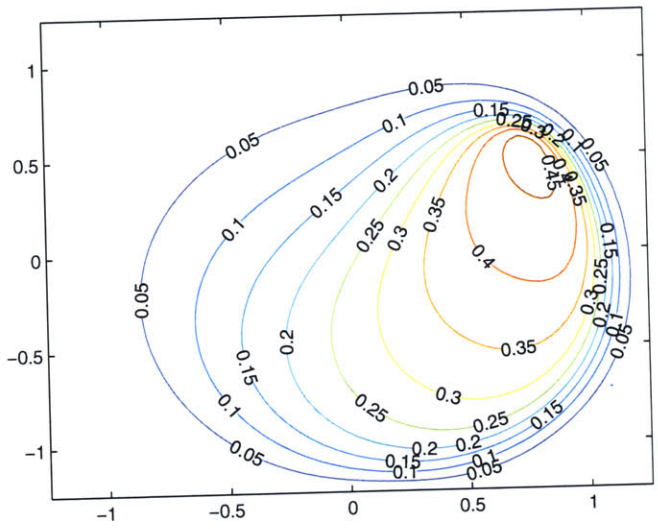

Figure 3-5: Contour plot of the DG solution for Two-Dimensional Buckley-Leverett equation at $T = 0.5$

$\mathcal{D} \equiv [0.05, 0.1]$, and the flux vector $\mathbf{f}(u) = (f_1(u), f_2(u))$ is given by

$$f_1(u) = \frac{u^2}{u^2 + (1-u)^2}, \qquad f_2(u) = f_1(u)(1 - 5(1-u)^2) \ . \tag{3.45}$$

The output $s(\mu, t)$ is evaluated as $s(\mu, t) = \ell(u(\mu, t))$ for $\ell(v) = \int_\Omega v$. The contour plot of the computed DG solution at the final time $T = 0.5$ is shown in Figure 3-5. The solutions is obtained with fourth-order finite element approximation space $X_h^{p=4}$ of dimension $\mathcal{N} = 12,000$, and $\nu = 0.05$.

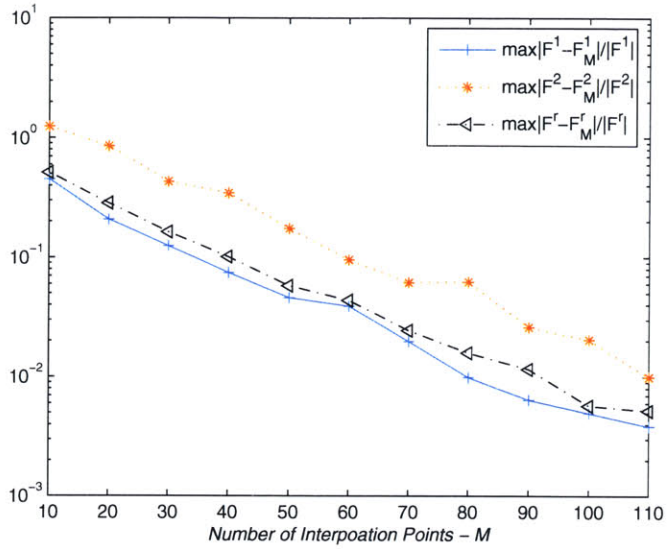

Figure 3-6: Approximation accuracy of nonlinear terms for Two-Dimensional Buckley-Leverett equation

Numerical Results-Function Formulation

The three nonlinear terms, f_1, f_2, $\hat{f}$, in the 2D Buckley-Leverett equation have to be specially approximated by the empirical interpolation method. Before this method is incorporated to the reduced-basis model of the whole system, its approximation accuracy has to be justified. In Figure 3-6 we compare the accuracy of the functions and their approximates. All the three functions can be approximated more accurately with more and more interpolation points being used.

Following the definitions in (3.42) and (3.43), we plot $\epsilon^s_{N,M,max,rel}$ in Figure 3-7 as a function of N and M, and $\epsilon^u_{N,M,max,rel}$ in Figure 3-8. The two figures show the same behavior: the errors converge as N increases, and level off at smaller and smaller values as we increase M. This is because when N is small, the dominating error is caused by the field variable u_N; when N is large enough such that the field variable is approximated more accurately, the errors in the nonlinear terms start to dominate. The final error level of a particular M is determined by the accuracy of the corresponding empirical interpolation approximation.

To verify that our RB approximation satisfy the accuracy level of interest, we use the *a posteriori* error estimator introduced in Section 3.6, and $\tau = 0.5$. The effectivities are presented in Table 3.4.

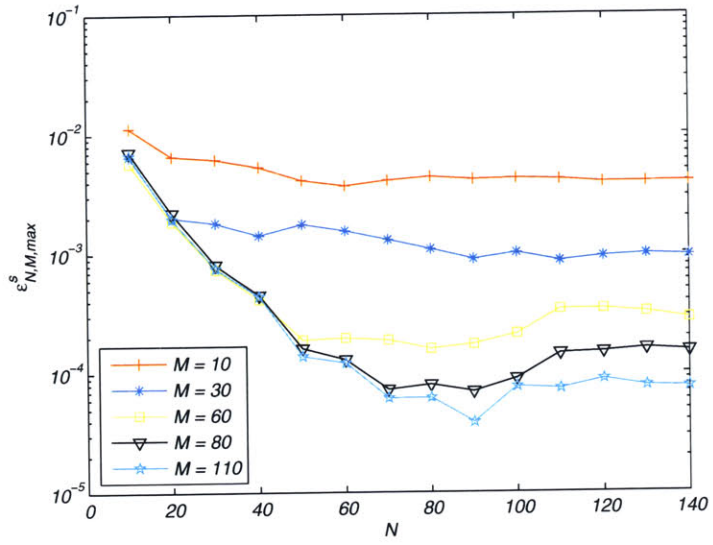

Figure 3-7: Convergence of the reduced-basis approximation output for Two-Dimensional Buckley-Leverett equation

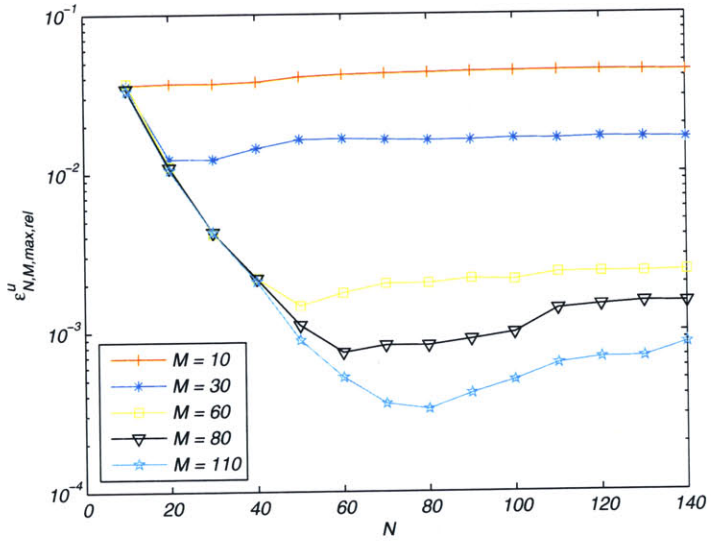

Figure 3-8: Convergence of the reduced-basis approximation solution for Two-Dimensional Buckley-Leverett equation

Table 3.4: Effectivites for Two-Dimensional Buckley-Leverett equation

N	M	$\Delta^s_{N,2N}$	$\eta^s_{N,M}$	$\Delta^u_{N,2N}$	$\eta^u_{N,M}$
10	20	2.0255×10^{-2}	2.2322	2.3682×10^{-4}	1.8748
20	30	4.5120×10^{-3}	2.7415	3.6648×10^{-5}	1.9501
30	30	3.9822×10^{-3}	2.0399	2.3300×10^{-5}	2.0425
40	40	1.4793×10^{-3}	2.1870	3.6034×10^{-6}	2.0102
50	40	1.2819×10^{-3}	2.1897	3.3151×10^{-6}	2.0217
60	50	7.2419×10^{-4}	3.1641	2.4356×10^{-6}	2.0579

Table 3.5: Online computational times (normalized) for Two-Dimensional Buckley-Leverett equation

N	M	*RBA*	*DG*
10	10	3.8905×10^{-3}	1
20	20	4.3953×10^{-3}	1
30	30	4.4730×10^{-3}	1
40	40	6.1853×10^{-3}	1
40	60	6.4143×10^{-3}	1
60	60	7.3889×10^{-3}	1

The mean effectivities are of order $O(1)$ as $\epsilon \to 0$.

The efficiency of the reduced-basis system is measured by the online computational times of each timestep. The values are normalized with respect to the computational time of direct calculation of the truth approximation output, i.e. DG approach. Significant saving has been achieved: A factor of more than 100 saving for the largest reduced-basis system in our experiments. Most significantly, it is also possible to use a much larger timestep in our RB system, without incurring any accuracy loss, which further speeds up the calculation of output $s_{N,M}(\mu, t_k)$.

Chapter 4

Extension to The Euler Equations

So far we have considered reduced-basis approximations for time-dependent parameterized PDEs of up to two-dimensional scalar problems. In this chapter, we will continue to extend the approach developed to systems of equations, and consider RB approximations to unsteady compressible Euler equations. We present here the function approximation formulation for the one-dimensional problem. The derivation of the residual approximation formulation and generalization to multi-dimensional problems is straightforward.

4.1 Problem Formulations

The one-dimensional Euler equations of compressible flows in conservative form are

$$\frac{\partial \mathbf{u}}{\partial t} + \frac{\partial \mathbf{F}(\mathbf{u})}{\partial x} = 0, \quad \text{in } \Omega \times (0, T] \tag{4.1}$$

with appropriate boundary conditions and initial condition $\mathbf{u}(x, t = 0) = \mathbf{u}_0(x)$. Here, the conservative state $\mathbf{u}$ and the inviscid flux vector $\mathbf{F}(\mathbf{u})$ are given by

$$\mathbf{u} = \begin{pmatrix} u^1 \\ u^2 \\ u^3 \end{pmatrix} = \begin{pmatrix} \rho \\ \rho v \\ \rho e \end{pmatrix}, \qquad \mathbf{F}(\mathbf{u}) = \begin{pmatrix} f_1(\mathbf{u}) \\ f_2(\mathbf{u}) \\ f_3(\mathbf{u}) \end{pmatrix} = \begin{pmatrix} \rho v \\ \rho v^2 + p \\ v(\rho e + p) \end{pmatrix}, \tag{4.2}$$

where ρ is the fluid density, v is the velocity, p is the pressure, and e is the total internal energy per unit mass. The perfect gas equation of state relates the static pressure p to components of the state vector $\mathbf{u}$ as

$$p = (\gamma - 1)\rho(e - v^2/2), \tag{4.3}$$

where γ is the ratio of specific heats of the fluid. The parameters we consider is the static pressure variation at outflow, which shall be denoted as μ and varies in the parameter space $\mathcal{D}$.

We now define the DG weak formulation for the governing equations (4.1) – (4.3). We assume that we are given a decomposition $\mathcal{T}_h$ of the domain Ω and associated function space X_h^p defined in Section 2.1. In addition, we introduce

$$Z_h^p = \left\{ \sigma \in \left(L^2(\Omega)\right)^3 \quad | \quad \sigma_i|_{T_h} \in P^p(T_h), \quad \forall T_h \in \mathcal{T}_h, \ 1 \le i \le 3 \right\} . \tag{4.4}$$

The weak formulation then takes the following form: find $\mathbf{u}_h = (u_h^1, u_h^2, u_h^3) \in Z_h^p$ such that

$$\sum_{T_h \in \mathcal{T}_h} \left\{ \int_{T_h} \frac{\partial \mathbf{u}_h}{\partial t} \mathbf{v}_h - \int_{T_h} \mathbf{F}(\mathbf{u}_h) \nabla \mathbf{v}_h + \int_{\partial T_h} \hat{\mathbf{F}}(\mathbf{u}_h, \mathbf{n}) \mathbf{v}_h \right\} = 0, \quad \forall \mathbf{v}_h \in Z_h^p \tag{4.5}$$

where $\hat{\mathbf{F}}(\mathbf{u}_h, \mathbf{n})$ is the numerical flux. The Roe flux function [38] is used here to define the numerical flux as

$$\hat{\mathbf{F}}(\mathbf{u}_h, \mathbf{n}) = \frac{1}{2} \left[\mathbf{F}(\mathbf{u}_h^+) + \mathbf{F}(\mathbf{u}_h^-) \right] \cdot \mathbf{n} - \frac{1}{2} |A| \left(\mathbf{u}_h^+ - \mathbf{u}_h^- \right) , \tag{4.6}$$

where $A = [\partial \mathbf{F}_i(\mathbf{u}_h^R)/\partial \mathbf{u}] \cdot \mathbf{n}$ is the Jacobian matrix evaluated at the Roe average state $\mathbf{u}_h^R$, and $|A| = S|\Lambda|S^{-1}$, S being the matrix of the right eigenvectors of A and $|\Lambda|$ being the diagonal matrix of the absolute eigenvalues of A.

Finally, by decomposing $\hat{\mathbf{F}}(\mathbf{u}_h, \mathbf{n}) = [\hat{f}_1(\mathbf{u}_h, \mathbf{n}), \hat{f}_2(\mathbf{u}_h, \mathbf{n}), \hat{f}_3(\mathbf{u}_h, \mathbf{n})]^T$, we can write (4.5) more explicitly as: for all $v_h \in X_h^p$, find $\mathbf{u}_h = (u_h^1, u_h^2, u_h^3) \in X_h^p \times X_h^p \times X_h^p$ such that

$$\begin{aligned}
\sum_{T_h \in \mathcal{T}_h} \int_{T_h} \frac{\partial u_h^1}{\partial t} v_h &= \sum_{T_h \in \mathcal{T}_h} \left\{ \int_{T_h} f_1(\mathbf{u}_h) \nabla v_h - \int_{\partial T_h} \hat{f}_1(\mathbf{u}_h, \mathbf{n}) v_h \right\}, \\
\sum_{T_h \in \mathcal{T}_h} \int_{T_h} \frac{\partial u_h^2}{\partial t} v_h &= \sum_{T_h \in \mathcal{T}_h} \left\{ \int_{T_h} f_2(\mathbf{u}_h) \nabla v_h - \int_{\partial T_h} \hat{f}_2(\mathbf{u}_h, \mathbf{n}) v_h \right\}, \\
\sum_{T_h \in \mathcal{T}_h} \int_{T_h} \frac{\partial u_h^3}{\partial t} v_h &= \sum_{T_h \in \mathcal{T}_h} \left\{ \int_{T_h} f_3(\mathbf{u}_h) \nabla v_h - \int_{\partial T_h} \hat{f}_3(\mathbf{u}_h, \mathbf{n}) v_h \right\} .
\end{aligned} \tag{4.7}$$

with the initial conditions $u_h^1(x;\mu;t=0) = u_{h0}^1(x)$, $u_h^2(x;\mu;t=0) = u_{h0}^2(x)$, and $u_h^3(x;\mu;t=0) = u_{h0}^3(x)$; here $u_{h0}^1(x), u_{h0}^2(x)$, and $u_{h0}^3(x)$ are the L^2-projection of $u_0^1(x)$, $u_0^2(x)$, and $u_0^3(x)$ on X_h^p, respectively. The FE approximation output is then given by

$$s_h(\mu,t) = \ell(u_h^1(\mu,t)) \ . \tag{4.8}$$

We use the fourth-order explicit RK scheme described in Section 2.2 to integrate the system (4.7)-(4.8) in time, thereby obtaining the truth approximations $\mathbf{u}_h(\mu,t_k)$ and $s_h(\mu,t_k), k=1,\ldots,K$.

4.2 Fully Discrete Equations

We begin by introducing several approximation spaces constructed upon the set of snapshots $\{\mathbf{u}_h(\tilde{\mu}_p), \tilde{\mu}_p \in \tilde{\mathcal{D}}, 1 \le p \le P\}$. We first apply the POD procedure to construct RB approximation spaces $\Phi_{N^1}^1 = \text{span}\{\phi_1^1,\ldots,\phi_{N^1}^1\}$ for u_h^1, $\Phi_{N^2}^2 = \text{span}\{\phi_1^2,\ldots,\phi_{N^2}^2\}$ for u_h^2, and $\Phi_{N^3}^3 = \text{span}\{\phi_1^3,\ldots,\phi_{N^3}^3\}$ for u_h^3. We then use POD and empirical interpolation procedures to construct collateral RB interpolation spaces $\Psi_{M^2}^2 = \text{span}\{\psi_1^2,\ldots,\psi_{M^2}^2\}$, $\Psi_{M^3}^3 = \text{span}\{\psi_1^3,\ldots,\psi_{M^3}^3\}$, and associated sets of interpolation points $T_{M^2}^2 = \{z_1^2,\ldots,z_{M^2}^2\}$, $T_{M^3}^3 = \{z_1^3,\ldots,z_{M^3}^3\}$ for the nonlinear functions $f_2(\mathbf{u}_h), f_3(\mathbf{u}_h)$, respectively; note that $f_1(\mathbf{u}_h) = u_h^2$ is linear and does not need the empirical interpolation treatment. Finally, in a similar manner, we build collateral RB interpolation spaces $\hat{\Psi}_{\hat{M}^1}^1 = \text{span}\{\hat{\psi}_1^1,\ldots,\psi_{\hat{M}^1}^1\}$, $\hat{\Psi}_{\hat{M}^2}^2 = \text{span}\{\hat{\psi}_1^2,\ldots,\hat{\psi}_{\hat{M}^2}^2\}$, $\hat{\Psi}_{\hat{M}^3}^3 = \text{span}\{\hat{\psi}_1^3,\ldots,\hat{\psi}_{\hat{M}^3}^3\}$, and associated sets of interpolation points $\hat{T}_{\hat{M}^1}^1 = \{\hat{z}_1^1,\ldots,\hat{z}_{\hat{M}^1}^1\}$, $\hat{T}_{\hat{M}^2}^2 = \{\hat{z}_1^2,\ldots,\hat{z}_{\hat{M}^2}^2\}$, $\hat{T}_{\hat{M}^3}^3 = \{\hat{z}_1^3,\ldots,\hat{z}_{\hat{M}^3}^3\}$ for the nonlinear functions $\hat{f}_1(\mathbf{u}_h,\mathbf{n}), \hat{f}_2(\mathbf{u}_h,\mathbf{n}), \hat{f}_3(\mathbf{u}_h,\mathbf{n})$, respectively; these functions are defined on the edges $\mathcal{E}(\mathcal{T}_h)$. For notational convenience, we assume that $N \equiv N^1 = N^2 = N^3$ and $M \equiv M^1 = M^2 = M^3 = \hat{M}^1 = \hat{M}^2 = \hat{M}^3$.

Applying a Galerkin projection to the system (4.7) and replacing the nonlinear functions by the coefficient function approximations, we obtain the reduced-order model: for any $\mu \in \mathcal{D}$, we evaluate

$$s_{N,M}(\mu,t) = \ell(u_{N,M}^1(\mu,t)) \ , \tag{4.9}$$

where $\mathbf{u}_{N,M}(\mu,t) = (u^1_{N,M}(\mu,t), u^2_{N,M}(\mu,t), u^3_{N,M}(\mu,t))^T \in \Phi^1_N \times \Phi^2_N \times \Phi^3_N$ satisfy

$$\begin{aligned}
\sum_{T_h\in\mathcal{T}_h}\int_{T_h}\frac{\partial u^1_{N,M}}{\partial t}v_N &= \sum_{T_h\in\mathcal{T}_h}\left\{\int_{T_h}u^2_{N,M}\nabla v_N - \int_{\partial T_h}\hat{f}^{\mathbf{u}_{N,M}}_{1,M}v_N\right\}, \quad \forall v_N\in\Phi^1_N \\
\sum_{T_h\in\mathcal{T}_h}\int_{T_h}\frac{\partial u^2_{N,M}}{\partial t}v_N &= \sum_{T_h\in\mathcal{T}_h}\left\{\int_{T_h}f^{\mathbf{u}_{N,M}}_{2,M}\nabla v_N - \int_{\partial T_h}\hat{f}^{\mathbf{u}_{N,M}}_{2,M}v_N\right\}, \quad \forall v_N\in\Phi^2_N \qquad (4.10)\\
\sum_{T_h\in\mathcal{T}_h}\int_{T_h}\frac{\partial u^3_{N,M}}{\partial t}v_N &= \sum_{T_h\in\mathcal{T}_h}\left\{\int_{T_h}f^{\mathbf{u}_{N,M}}_{3,M}\nabla v_N - \int_{\partial T_h}\hat{f}^{\mathbf{u}_{N,M}}_{3,M}v_N\right\}, \quad \forall v_N\in\Phi^3_N.
\end{aligned}$$

Here $f^{\mathbf{u}_{N,M}}_{2,M}, f^{\mathbf{u}_{N,M}}_{3,M}, \hat{f}^{\mathbf{u}_{N,M}}_{1,M}, \hat{f}^{\mathbf{u}_{N,M}}_{2,M}, \hat{f}^{\mathbf{u}_{N,M}}_{3,M}$ are the coefficient function approximations to the nonlinear functions $f_2(\mathbf{u}_{N,M}), f_3(\mathbf{u}_{N,M}), \hat{f}_1(\mathbf{u}_{N,M}), \hat{f}_2(\mathbf{u}_{N,M},\mathbf{n}), \hat{f}_3(\mathbf{u}_{N,M},\mathbf{n})$, respectively.

To arrive at the matrix-vector form for the system (4.9)-(4.10), we first expand the RB approximations $u^1_{N,M}(\mu,t)\in\Phi^1_N, u^2_{N,M}(\mu,t)\in\Phi^2_N$, and $u^3_{N,M}(\mu,t)\in\Phi^3_N$ as

$$u^1_{N,M}(\mu,t) = \sum_{n=1}^{N}\alpha^1_n(\mu,t)\phi^1_n, \quad u^2_{N,M}(\mu,t) = \sum_{n=1}^{N}\alpha^2_n(\mu,t)\phi^2_n, \quad u^3_{N,M}(\mu,t) = \sum_{n=1}^{N}\alpha^3_n(\mu,t)\phi^3_n\ . \quad (4.11)$$

It then follows that our coefficient function approximations $f^{\mathbf{u}_{N,M}}_{2,M}, f^{\mathbf{u}_{N,M}}_{3,M}, \hat{f}^{\mathbf{u}_{N,M}}_{1,M}, \hat{f}^{\mathbf{u}_{N,M}}_{2,M}, \hat{f}^{\mathbf{u}_{N,M}}_{3,M}$ are given by

$$\begin{aligned}
f^{\mathbf{u}_{N,M}}_{2,M}(x;\mu,t) &= \textstyle\sum_{m=1}^{M}\beta^2_m(\mu,t)\psi^2_m(x), \quad B^2\beta^2(\mu,t) = f_2\big(D^{12}\alpha^1(\mu,t), D^{22}\alpha^2(\mu,t), D^{32}\alpha^3(\mu,t)\big)\\
f^{\mathbf{u}_{N,M}}_{3,M}(x;\mu,t) &= \textstyle\sum_{m=1}^{M}\beta^3_m(\mu,t)\psi^3_m(x), \quad B^3\beta^3(\mu,t) = f_3\big(D^{13}\alpha^1(\mu,t), D^{23}\alpha^2(\mu,t), D^{33}\alpha^3(\mu,t)\big)\\
\hat{f}^{\mathbf{u}_{N,M}}_{1,M}(x;\mu,t) &= \textstyle\sum_{m=1}^{M}\hat{\beta}^1_m(\mu,t)\hat{\psi}^1_m(x), \quad \hat{B}^1\hat{\beta}^1(\mu,t) = \hat{f}_1\big(\hat{D}^{11}\alpha^1(\mu,t), \hat{D}^{21}\alpha^2(\mu,t), \hat{D}^{31}\alpha^3(\mu,t), \hat{n}^1\big)\\
\hat{f}^{\mathbf{u}_{N,M}}_{2,M}(x;\mu,t) &= \textstyle\sum_{m=1}^{M}\hat{\beta}^2_m(\mu,t)\hat{\psi}^2_m(x), \quad \hat{B}^2\hat{\beta}^2(\mu,t) = \hat{f}_2\big(\hat{D}^{12}\alpha^1(\mu,t), \hat{D}^{22}\alpha^2(\mu,t), \hat{D}^{32}\alpha^3(\mu,t), \hat{n}^2\big)\\
\hat{f}^{\mathbf{u}_{N,M}}_{3,M}(x;\mu,t) &= \textstyle\sum_{m=1}^{M}\hat{\beta}^3_m(\mu,t)\hat{\psi}^3_m(x), \quad \hat{B}^3\hat{\beta}^3(\mu,t) = \hat{f}_3\big(\hat{D}^{13}\alpha^1(\mu,t), \hat{D}^{23}\alpha^2(\mu,t), \hat{D}^{33}\alpha^3(\mu,t), \hat{n}^3\big)
\end{aligned}$$

where for $1\le i,m\le M$, $1\le n\le N$,

$$B^2_{im} = \psi^2_m(z^2_i), \quad D^{12}_{in} = \phi^1_n(z^2_i), \quad D^{22}_{in} = \phi^2_n(z^2_i), \quad D^{32}_{in} = \phi^3_n(z^2_i), \qquad (4.12)$$

$$B^3_{im} = \psi^3_m(z^2_i), \quad D^{13}_{in} = \phi^1_n(z^3_i), \quad D^{23}_{in} = \phi^2_n(z^3_i), \quad D^{33}_{in} = \phi^3_n(z^3_i), \qquad (4.13)$$

$$\hat{B}^1_{im} = \hat{\psi}^1_m(\hat{z}^1_i), \quad \hat{D}^{11}_{in} = \phi^1_n(\hat{z}^1_i), \quad \hat{D}^{21}_{in} = \phi^2_n(\hat{z}^1_i), \quad \hat{D}^{31}_{in} = \phi^3_n(\hat{z}^1_i), \quad \hat{n}^1_i = \mathbf{n}(\hat{z}^1_i) \tag{4.14}$$

$$\hat{B}^2_{im} = \hat{\psi}^2_m(\hat{z}^2_i), \quad \hat{D}^{12}_{in} = \phi^1_n(\hat{z}^2_i), \quad \hat{D}^{22}_{in} = \phi^2_n(\hat{z}^2_i), \quad \hat{D}^{32}_{in} = \phi^3_n(\hat{z}^2_i), \quad \hat{n}^2_i = \mathbf{n}(\hat{z}^2_i) \tag{4.15}$$

$$\hat{B}^3_{im} = \hat{\psi}^3_m(\hat{z}^3_i), \quad \hat{D}^{13}_{in} = \phi^1_n(\hat{z}^3_i), \quad \hat{D}^{23}_{in} = \phi^2_n(\hat{z}^3_i), \quad \hat{D}^{33}_{in} = \phi^3_n(\hat{z}^3_i), \quad \hat{n}^3_i = \mathbf{n}(\hat{z}^3_i). \tag{4.16}$$

Inserting the representations (4.11) and our coefficient-function approximations into (4.10) yields

$$\sum_{j=1}^{N}\sum_{T_h\in\mathcal{T}_h}\int_{T_h}\phi^1_j\phi^1_i\dot{\alpha}^1_j(\mu,t) = \sum_{k=1}^{N}\sum_{T_h\in\mathcal{T}_h}\int_{T_h}\phi^2_k\nabla\phi^1_i\alpha^2_k(\mu,t) - \sum_{m=1}^{M}\sum_{T_h\in\mathcal{T}_h}\int_{\partial T_h}\hat{\psi}^1_m\phi^1_i\hat{\beta}^1_m(\mu,t), \quad 1\le i\le N$$

$$\sum_{j=1}^{N}\sum_{T_h\in\mathcal{T}_h}\int_{T_h}\phi^2_j\phi^2_i\dot{\alpha}^2_j(\mu,t) = \sum_{k=1}^{M}\sum_{T_h\in\mathcal{T}_h}\int_{T_h}\psi^2_k\nabla\phi^2_i\beta^2_k(\mu,t) - \sum_{m=1}^{M}\sum_{T_h\in\mathcal{T}_h}\int_{\partial T_h}\hat{\psi}^2_m\phi^2_i\hat{\beta}^2_m(\mu,t), \quad 1\le i\le N$$

$$\sum_{j=1}^{N}\sum_{T_h\in\mathcal{T}_h}\int_{T_h}\phi^3_j\phi^3_i\dot{\alpha}^3_j(\mu,t) = \sum_{k=1}^{M}\sum_{T_h\in\mathcal{T}_h}\int_{T_h}\psi^3_k\nabla\phi^3_i\beta^3_k(\mu,t) - \sum_{m=1}^{M}\sum_{T_h\in\mathcal{T}_h}\int_{\partial T_h}\hat{\psi}^3_m\phi^3_i\hat{\beta}^3_m(\mu,t), \quad 1\le i\le N$$

in terms of which the RB output can be subsequently calculated as

$$s_{N,M}(\mu,t) = \sum_{n=1}^{N}\alpha^1_n(\mu,t)\ell(\phi^1_i)\ . \tag{4.17}$$

It remains to develop the offline-online procedure for the rapid evaluation of $s_{N,M}(\mu,t)$.

4.3 Offline/Online Procedure

Let us first introduce the following matrices

$$A^1_{in} = \sum_{T_h\in\mathcal{T}_h}\int_{T_h}\phi^1_n\phi^1_i, \qquad A^2_{in} = \sum_{T_h\in\mathcal{T}_h}\int_{T_h}\phi^2_n\phi^2_i, \qquad A^3_{in} = \sum_{T_h\in\mathcal{T}_h}\int_{T_h}\phi^3_n\phi^3_i, \tag{4.18}$$

$$\begin{aligned} C^1_{in} &= \sum_{T_h\in\mathcal{T}_h}\int_{T_h}\phi^2_n\nabla\phi^1_i, & \hat{C}^1_{im} &= \sum_{T_h\in\mathcal{T}_h}\int_{\partial T_h}\hat{\psi}^1_m\phi^1_i, \\ C^2_{im} &= \sum_{T_h\in\mathcal{T}_h}\int_{T_h}\psi^2_m\nabla\phi^2_i, & \hat{C}^2_{im} &= \sum_{T_h\in\mathcal{T}_h}\int_{\partial T_h}\hat{\psi}^2_m\phi^2_i, \\ C^3_{im} &= \sum_{T_h\in\mathcal{T}_h}\int_{T_h}\psi^3_m\nabla\phi^3_i, & \hat{C}^3_{im} &= \sum_{T_h\in\mathcal{T}_h}\int_{\partial T_h}\hat{\psi}^3_m\phi^3_i, \end{aligned} \tag{4.19}$$

for $1 \le i, n \le N, 1 \le m \le M$; and

$$E^1 = (A^1)^{-1}(C^1), \qquad E^2 = (A^2)^{-1}(C^2)(B^2)^{-1}, \qquad E^3 = (A^3)^{-1}(C^3)(B^3)^{-1} \tag{4.20}$$

$$\hat{E}^1 = (A^1)^{-1}(\hat{C}^1)(\hat{B}^1)^{-1}, \qquad \hat{E}^2 = (A^2)^{-1}(\hat{C}^2)(\hat{B}^2)^{-1}, \qquad \hat{E}^3 = (A^3)^{-1}(\hat{C}^3)(\hat{B}^3)^{-1} \ . \tag{4.21}$$

It thus follows from (4.17) and (4.12)-(4.16) that we obtain the ODE system

$$\begin{aligned}
\dot{\alpha}^1(\mu,t) &= E^1\alpha^2 - \hat{E}^1\hat{f}_1\big(\hat{D}^{11}\alpha^1, \hat{D}^{21}\alpha^2, \hat{D}^{31}\alpha^3, \hat{n}^1\big) \\
\dot{\alpha}^2(\mu,t) &= E^2 f_2\big(D^{12}\alpha^1, D^{22}\alpha^2, D^{32}\alpha^3\big) - \hat{E}^2\hat{f}_2\big(\hat{D}^{12}\alpha^1, \hat{D}^{22}\alpha^2, \hat{D}^{32}\alpha^3, \hat{n}^2\big) \\
\dot{\alpha}^3(\mu,t) &= E^3 f_3\big(D^{13}\alpha^1, D^{23}\alpha^2, D^{33}\alpha^3\big) - \hat{E}^3\hat{f}_3\big(\hat{D}^{13}\alpha^1, \hat{D}^{23}\alpha^2, \hat{D}^{33}\alpha^3, \hat{n}^3\big),
\end{aligned} \tag{4.22}$$

with the initial conditions $\alpha^1(\mu, t=0) = \alpha_0^1$, $\alpha^2(\mu, t=0) = \alpha_0^2$, and $\alpha^3(\mu, t=0) = \alpha_0^3$, where

$$\alpha_{0i}^1 = (\phi_i^1, u_{h0}^1), \qquad \alpha_{0i}^2 = (\phi_i^2, u_{h0}^2), \qquad \alpha_{0i}^3 = (\phi_i^3, u_{h0}^3), \quad 1 \le i \le N \ . \tag{4.23}$$

The RB output is thus calculated by

$$s_{N,M}(\mu,t) = L^T\alpha^1(\mu,t), \tag{4.24}$$

where $L_i = \ell(\phi_i^1), 1 \le i \le N$. By using the 4^{th} order RK scheme to solve the system (4.22), we obtain the RB approximations $s_{N,M}(\mu,t_k)$ to $s_h(\mu,t_k)$ for $k = 0,\ldots,K$. The procedure for the rapid evaluation of $s_{N,M}(\mu,t_k), 0 \le k \le K$, is described below.

In the offline stage — performed *once* — we form and *store* the parameter-*independent* quantities $\alpha_0^1, \alpha_0^2, \alpha_0^3,,\ \hat{n}^1, \hat{n}^2, \hat{n}^3,\ D^{12}, D^{22}, D^{32},\ D^{13}, D^{23}, D^{33},\ \hat{D}^{11}, \hat{D}^{21}, \hat{D}^{31},\ \hat{D}^{12}, \hat{D}^{22}, \hat{D}^{32},\ \hat{D}^{13}, \hat{D}^{23}, \hat{D}^{33},$ $E^1, E^2, E^3,\ \hat{E}^1, \hat{E}^2, \hat{E}^3$. In the online stage — performed *many* times, for each new value of $\mu \in \mathcal{D}$ — we simply solve (4.22) for $\alpha^1(\mu,t_k), \alpha^2(\mu,t_k), \alpha^3(\mu,t_k)$ at cost $O\left(4\left(20MN + N^2\right)\right)$, and evaluate $s_{N,M}(\mu,t_k)$ from (4.24) at cost $O(N)$; (note that the 4^{th} order RK scheme requires four evaluations of the right-hand side of (4.22) and each of evaluation takes $O\left(20MN + N^2\right)$). The operation count for the online stage is thus $O\left(4K\left(20MN + N^2\right)\right)$. The online complexity is again *independent* of $\mathcal{N}$.

Finally, the *a posteriori* error estimator $\Delta_{N,M}^s(\mu,t_k)$ can be obtained from (3.25), which in turn

necessitates calculation of $s_{2N,2M}(\mu, t_k)$. The overall computational cost is thus increased by a factor of 4.

4.4 Numerical Examples

4.4.1 Problem Description

We solve a quasi-1D Euler equations for unsteady flow in a duct of cross-section $a(x)$, on the domain $\Omega \equiv]0,1[$, defined as

$$a(x)\frac{\partial \mathbf{u}}{\partial t} + \frac{\partial}{\partial x}(a(x)\mathbf{F}(\mathbf{u})) - \frac{da(x)}{dx}\mathbf{p} = 0, \quad \text{in } \Omega \times (0,1] \tag{4.25}$$

with the conservative state $\mathbf{u}$ and the inviscid flux vector $\mathbf{F}(\mathbf{u})$ as shown by (4.2), and $\mathbf{p} = (0, p, 0)^T$. The geometry of the duct is defined by

$$a(x) = \begin{cases} 1, & 0 \le x \le 0.1 \\ 1 - 0.3\cos^2(\pi(x-0.5)/0.8), & 0.1 < x < 0.9 \\ 1, & 0.9 \le x \le 1\ . \end{cases} \tag{4.26}$$

The initial conditions are given by

$$\rho_0(x) = a(x), \qquad v_0(x) = 1, \qquad e_0(x) = 20.3413\ . \tag{4.27}$$

The boundary condition is the static pressure at outlet $p_{\text{ex}} = 7.9365 + \delta\sin(2\pi t)$, where δ is the magnitude of a small sinusoidal perturbation of the static pressure at outlet. Here $\mu \equiv \delta$ is the only parameter of interest and varies in the range $\mathcal{D} \equiv [0, 0.5]$. Note that the case $\delta = 0$ results in steady flow. The output $s(\mu, t)$ is evaluated as $s(\mu, t) = \ell(\rho(\mu, t))$ for $\ell(v) = \int_\Omega v$.

The Mach number of the DG solutions at different time instances $t = (0.2, 0.4, 0.6, 0.8, 1)$ is shown in Figure (4-1). These solutions are obtained with fifth-order finite element approximation space $X_h^{p=5}$ of dimension $\mathcal{N} = 1000$, and for several $\delta = (0, 0.2, 0.4, 0.5)$.

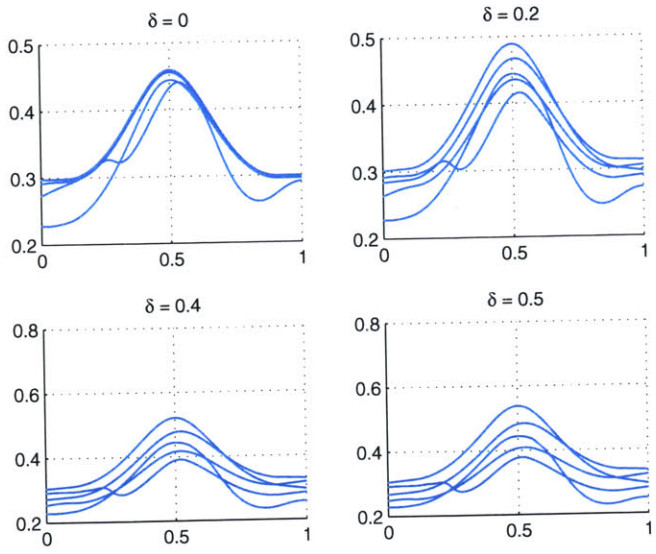

Figure 4-1: DG solution for One-Dimensional Euler equation at $T = 1.0$

Table 4.1: Maximum relative errors of output and solutions for One-Dimensional Euler equation

N	M	$\epsilon^s_{N,M,max,rel}$	$\epsilon^{u^1}_{N,M,max,rel}$	$\epsilon^{u^2}_{N,M,max,rel}$	$\epsilon^{u^3}_{N,M,max,rel}$
10	20	3.3013×10^{-4}	3.6795×10^{-3}	8.5286×10^{-3}	3.9197×10^{-3}
15	24	8.5233×10^{-5}	1.5534×10^{-3}	2.7204×10^{-3}	1.7041×10^{-3}
20	28	4.2908×10^{-5}	8.5071×10^{-4}	1.6375×10^{-3}	8.8667×10^{-4}
20	32	4.1637×10^{-5}	8.1511×10^{-4}	1.4605×10^{-3}	8.6825×10^{-4}
25	40	1.8822×10^{-5}	4.4571×10^{-4}	7.6843×10^{-4}	4.5668×10^{-4}
30	44	1.1642×10^{-5}	3.5110×10^{-4}	6.8175×10^{-4}	3.7008×10^{-4}

4.4.2 Numerical Results-Function Formulation

We now present the numerical results of reduced-basis method for unsteady quasi-1D Euler equations. The convergence of the reduced-basis approximation of output and field variable solutions are tabulated in Table 4.1, note that the (N, M) pairs roughly correspond to the "knees" of what would have been observed in the N–M-convergence curves. Not surprisingly, again the output converges faster than that of the field variable solutions. Moreover, the three variable solutions converge at almost the same rate.

Next, the *a posterior* error estimators and the effectivities of the output approximation as well as solution approaximations are tabulated in Table 4.2. As $\epsilon \rightarrow 0$,the mean effectivities is of order

Table 4.2: Error estimators of output and solutions for One-Dimensional Euler equation

N	M	$\Delta^s_{N,M}$	$\Delta^{u^1}_{N,M}$	$\Delta^{u^2}_{N,M}$	$\Delta^{u^3}_{N,M}$
10	20	4.1570×10^{-2}	5.5542×10^{-3}	1.8432×10^{-2}	1.4738×10^{-1}
15	24	1.1829×10^{-2}	2.2608×10^{-3}	6.2198×10^{-2}	6.1518×10^{-2}
20	28	5.6966×10^{-3}	1.3240×10^{-3}	3.4746×10^{-3}	3.4020×10^{-2}
20	32	5.5078×10^{-3}	1.3197×10^{-4}	3.4706×10^{-3}	3.3864×10^{-2}
25	40	2.9277×10^{-3}	7.6268×10^{-4}	1.8912×10^{-3}	1.9222×10^{-2}
30	44	1.8947×10^{-3}	6.4576×10^{-4}	1.6698×10^{-3}	1.6713×10^{-2}

Table 4.3: Effectivities of output and solutions for One-Dimensional Euler equation

N	M	$\eta^s_{N,M}$	$\eta^{u^1}_{N,M}$	$\eta^{u^2}_{N,M}$	$\eta^{u^3}_{N,M}$
10	20	2.3444	2.4053	2.4988	2.3711
15	24	2.1692	2.2511	2.2440	2.2583
20	28	2.5113	2.4178	2.5411	2.9331
20	32	2.9992	2.5743	2.7865	3.0169
25	40	2.8828	3.0672	3.3748	4.1792
30	44	5.1459	3.1014	2.9913	2.9692

$O(1)$.

The computational savings obtained by the use of the reduced-basis approximation in one dimensional problem are not significant. In fact, the offline cost of the reduced basis approach makes it uninteresting in this case. This situation will be clearly different when we consider the two and three dimensional problem, or one dimensional problem with larger finite element approximation space (i.e. larger $\mathcal{N}$). Moreover, since a larger timestep can be used in the RB approximation, the *total* online computational saving can be more significant.

Table 4.4: Online computational times (normalized) for One-Dimensional Euler equation (per timestep)

N	M	*RBA*	*DG*
10	20	0.5099	1
15	24	0.5280	1
20	28	0.5584	1
20	32	0.5586	1
25	40	0.6124	1
30	44	0.6626	1

Chapter 5

Conclusion

5.1 Summary

The goal of this thesis has been the development of reduced-basis approximations of the solution and output of nonlinear time-dependent parameterized convection-diffusion equations and *a posterior* error estimators to certify the approximated results. The developed method has also been extended to the quasi one-dimensional Euler equations for unsteady flow.

We began by introducing the primary numerical method used to solve our targeted PDEs, i.e., Runge-Kutta Discontinuous Galerkin (RKDG) method. While pursuing high-order accuracy, local conservativity, and high parallelizability, the RKDG method introduces additional highly nonlinear numerical flux terms to the weak formulation, on top of the existing nonlinear functions of the PDEs. Conventional Galerkin approximation methods can no longer handle these nonlinear terms efficiently. To this end, we proposed an empirical interpolation approximation method to tackle this problem. For a general parameter-dependent nonlinear function, the empirical interpolation method aims to construct an inexpensive approximation via reduced-basis space and associated set of interpolation points, known as cofficient-function approximation, which further enables efficient offline-online decomposition.

Instead of using Lagrangian bases selected by a greedy algorithm procedure for the field variable approximation, we used the POD approach which is known to concentrate the most information within the fewest number of basis vectors, at the same time, produces a basis which is already orthonormal. The empirical interpolation approximation for the nonlinear terms of the field variable

is then incorporated into our reduced-basis model.

The two numerical examples presented in Chapter 3 served two purposes: (*i*) The one-dimensional viscous Burger's equation, which contains low order nonlinear function, justifies the accuracy and efficiency of empirical interpolation method while handling nonlinear terms, as compared with conventional Galerkin approximation method; (*ii*) The two-dimensional Buckley-Leverett equation, which contains high order nonlinear functions and complicated nonlinear numerical flux terms while solved with RKDG method, can be efficiently handled by reduced-basis model incorporated with empirical interpolation approximation. *A posteriori* error estimators proposed for the nonlinear time-dependent parameterized convection-diffusion problems certified that our reduced-basis model could achieve the desired accuracy level.

We further extended our reduced-basis model to handle systems of equations. We targeted the quasi one-dimensional unsteady compressible Euler equations, and the numerical results verified the accuracy of the reduced-basis approximation.

5.2 Future Work

The successful development and implementation of the reduced-basis model for nonlinear time-dependent parameterized convection-diffusion equations in this thesis suggests another topic of research, i.e., to further extend the model to handle problems with higher dimensions and more degrees of freedom, for example, unsteady Navier-Stokes equation.

The two reduced-basis formulations proposed in this thesis — function formulation and residual formulation – are both proven to be numerically accurate, while the residual formulation is believed to be simpler in terms of implementation but less stable for certain configuration of dimensions of the reduced-basis model. This suggests another direction of improvement for future work.

So far, the choice for the size of the reduced-basis model for a particular problem is purely empirical, which might depend on many factors, for example, initial condition, geometry, parameter space, and time span. The optimal dimensions for the reduced-basis models are hardly obtainable beforehand. An interesting question is thus to find the "best" choices for N and M which minimize the computational cost for a desired approximation accuracy.

For complicated parameterized PDEs, it is always of great interest to solve the inverse problem. Efficient and accurate reduced-basis models make it possible and lay the groundwork for this

problem. However, a lot of practical issues still needed to be addressed.

Bibliography

[1] P. Stern B. O. Almroth and F. A. Brogan. Automatic choice of global shape functions in structural analysis. *AIAA Journal*, 16:525–528, May 1978.

[2] Z. J. Bai. Krylov subspace techniques for reduced-order modeling of large-scale dynamical sysmtems. *Applied Numerical Mathematics*, 43(1), 2002.

[3] E. Balmes. Parametric families of reduced finite element models: Theory and applications. *Mechanical Systems and Signal Processing*, 10(4):381–394, 1996.

[4] E. Balmes. Parametric families of reduced finite element models: Theory and applications. *Mechanical Systems and Signal Processing*, 10(4):381–394, 1996.

[5] M. Barrault, N. C. Nguyen, Y. Maday, and A. T. Patera. An "empirical interpolation" method: Application to efficient reduced-basis discretization of partial differential equations. *C. R. Acad. Sci. Paris, Série I.*, 339:667–672, 2004.

[6] A. Barrett and G. Reddien. On the reduced basis method. *Z. Angew. Math. Mech.*, 75(7):543–549, 1995.

[7] F. Bassi and S. Rebay. A high-order accurate discontinuous finite element method for the numerical solution of the compressible navier-stokes equations. *J. Comput. Phys.*, 131(2):267–279, 1997.

[8] J. Chen and S-M. Kang. Model-order reduction of nonlinear mems devices through arclength-based karhunen-loéve decomposition. In *Proceedings of the IEEE international Symposium on Circuits and Systems*, volume 2, pages 457–460, 2001.

[9] Y. Chen and J. White. A quadratic method for nonlinear model order reduction. In *Proceedings of the Internaional Conference on Modeling and Simulation of Microsysmtems*, pages 477–480, 2000.

[10] M. Chou and J. White. Efficient formulation and model-order reduction for the transient simulation of three-dimensional vlsi interconnect. In *IEEE Transactions On Computer-Aided Design of Integrated Circuit and Systems*, volume 16, pages 1454–1476, 1997.

[11] Bernardo Cockburn, George Karniadakis, and Chi-Wang Shu. *Discontinuous Galerkin Methods: Theory, Compuration and Applications.* Lecture Notes in Computational Science and Engineering. Springer, New York, Berlin, Heidelberg, 2000.

[12] Bernardo Cockburn and Chi-Wang Shu. Runge-kutta discontinuous galerkin methods for convection-dominated problems. *J. Sci. Comput.*, 16(3):173–261, 2001.

[13] E. Michielssen D. S. Weile and K. Gallivan. Reduced-order modeling of multiscreen frequency-selective surfaces using krylov-based rational interpolation. *IEEE Transactions on Antennas and Propagation*, 49(5):801–813, May 2001.

[14] Earl H. Dowell and Kenneth C. Hall. Modeling of fluid structure interaction. *Annu. Rev. Fluid. Mech.*, 33:445–490, 2001.

[15] M. Brons E. A. Christensen and J. N. Sorensen. Evaluation of proper orthogonal decomposition-based decomposition techniques applied the parameter-dependent nonturbulent flows. *SIAM J. Scientific Computing*, 21(4):1419 -1434, 2000.

[16] J. P. Fink and W. C. Rheinboldt. On the error behavior of the reduced basis technique for nonlinear finite element approximations. *Z. Angew. Math. Mech.*, 63:21–28, 1983.

[17] M. A. Grepl, Y. Maday, N. C. Nguyen, and A. T. Patera. Efficient reduced-basis treatment of nonaffine and nonlinear partial differential equations. *M2AN (Math. Model. Numer. Anal.)*, 2006. Submitted.

[18] E.J. Grimme. *Krylov Projection Methods for Model Reduction.* PhD thesis, University of Illinois at Urbana-Champain, 1997.

[19] M. D. Gunzburger. Finite element methods for viscous incompressible flows: A guide to theory, practice, and algorithms. *Z. Angew. Math. Mech.*, 63:21–28, 1983.

[20] K. Ito and S. S. Ravindran. A reduced-order method for simulation and control of fluid flows. *Journal of Computational Physics*, 143(2):403–425, July 1998.

[21] D. Rovas K. Veroy and A. T. Patera. *A posteriori* error estimation for reduced-basis approximation of parametrized elliptic coercive partial differential equations: "convex inverse" bound conditions. *Control, Optimisation and Calculus of Variations*, 8:1007–1028, June 1987. Special Volume: A tribute to J.-L. Lions.

[22] D. V. Rovas K. Veroy, C. Prud'homme and A. T. Patera. *A posteriori* error bounds for reduced-basis approximation of parametrized noncoercive and nonlinear elliptic partial differential equations (aiaa paper 2003-3847). In *Proceedings of the 16th AIAA Computational Fluid Dynamics Conference*, June 2003.

[23] G. Lassaux and K. Willcox. Model reduction for active control design using multi-point arnoldi methods (AIAA Paper 2003-0616). In *Proceedings of the 41st Aerospace Sciences Meeting and Exibit*, January 2003.

[24] J. Lumley and P. Blossey. Control of turbulence. *Annu. Rev. Fluid. Mech.*, 30:311–327, 1998.

[25] K. Veroy A. T. Patera M. A. Grepl, N. C. Nguyen and G. R. Liu. Certified rrapid solution of parametrized partial differential equations for real-time applications. In *Proceedings of the 2nd Sandia Workshop of PDE-Constrained Optimization: Towards Real-Time and On-Line PDE-Constrained Optimization.* SIAM Computational Science and Engineering Book Series, 2004. Submitted.

[26] L. Machiels, Y. Maday, I. B. Oliveira, A. T. Patera, and D. V. Rovas. Output bounds for reduced-basis approximations of symmetric positive definite eigenvalue problems. *C. R. Acad. Sci. Paris, Série I*, 331(2):153–158, July 2000.

[27] M. Meyer and H. G. Matthies. Efficient model reduction in non-linear dynamics using the karhunen-loève expansion and dual-weighted-residual methods. *Computational Mechanics*, 31(1-2):179–191, May.

[28] N. C. Nguyen, K. Veroy, and A. T. Patera. Certified real-time solution of parametrized partial differential equations. In *Handbook of Materials Modeling*, pages 1523–1558. Springer.

[29] A. K. Noor and J. M. Peters. Reduced basis technique for nonlinear analysis of structures. *AIAA Journal*, 18(4):455–462, April 1980.

[30] S. Lall P. Krysl and J. E. Marsden. Dimensional model reduction in non-linear finite element dynamics of solids and structures. *International Journal for Numerical Methods in Engineering*, 51:479–504, 2001.

[31] P. Persson and J. Peraire. An efficient low memory implicit dg algorithm for time dependent problems. In *44th AIAA Aerospace Sciences Meeting*, pages AIAA–2006–0113, Reno, Neveda, 2006.

[32] J. S. Peterson. The reduced basis method for incompressible viscous flow calculations. *SIAM J. Sci. Stat. Comput.*, 10(4):777–786, July 1989.

[33] J. R. Phillips. Projection-based approaches for model reduction of weakly nonlinear systems, time-varying systems. In *IEEE Transactions on Computer-Aided Design of Integrated Circuit and Systems*, volume 22, pages 171–187, 2003.

[34] T. A. Porsching. Estimation of the error in the reduced-basis method solution of nonlinear equations. *Mathematics of Computations*, 45(172):487–496, October 1985.

[35] C. Prud'homme, D. Rovas, K. Veroy, Y. Maday, A. T. Patera, and G. Turinici. Reliable real-time solution of parametrized partial differential equations: Reduced-basis output bound methods. *Journal of Fluids Engineering*, 124(1):70–80, March 2002.

[36] M. Rewienski and J. White. A trajectory piecewise-linear approach to model order reduction and fast simulation of nonlinear circuits and micromachined devices. In *IEEE Transactions on Computer-Aided Design of Integrated Circuit and Systems*, volume 22, pages 155–170, 2003.

[37] W. C. Rheinboldt. On the theory and error estimation of the reduced-basis method for multi-parameter problems. *Nonlinear Analysis, theory, Methods and Applications*, 21(11):849–858, 1993.

[38] P. L. Roe. Approximate riemann solvers, parameter vectors, and difference schemes. *Computational Physics*, 43:357–372, 1981.

[39] J. M. A. Scherpen. Balancing for nonlinear systems. *Systems and Control Letters*, 21:143–153, 1993.

[40] L. Sirovich. Turbulence and the dynamics of coherent structures, part 1: Coherent structures. *Quarterly of Applied Mathematics*, 45(3):561–571, October 1987.

[41] M. Damodaran T. T. Bui and K. Wilcox. Proper orthogonal decomposition extensions for parametric applications in transonic aerodynamics (aiaa paper 2003-4213). In *Proceedings of the 15th AIAA Computational Fluid Dynamics Conference*, pages AIAA–2006–0113, June 2006.

[42] K. Veroy and A. T. Patera. Certified real-time solution of the parametrized steady incompressible navier-stokes equations; rigorous reduced-basis *a posterior* error bounds. *International Journal for Numerical Methods in Fluids*, 47:773–788, 2005.

[43] F. Wang and J. White. Automatic model order reduction of a microdevice using the arnoldi approch. In *Proceedings of the International Mechanical Engineering Congress and Exposition*, pages 527–530, 1998.

[44] K. Willcox and J. Peraire. Balanced model reduction via the proper orthogonal decomposition. In *15th AIAA Computational Fluid Dynamics Conference*. AIAA, June 2001.

[45] K. Willcox, J. Peraire, and J. White. An arnoldi approach for generation of reduced-order models for turbomachinery. *Computers and Fluids*, 31(3):369–389, 2002.

[46] T. Patera Y. Maday and G. Turinici. Global *a priori* convergence theory for reduced-basis approximation of single-parameter sysmmetric coercive elliptic partial differential equations. *C. R. Acad. Sci. Paris, Série I*, 335(3):289–294, 2002.